

Riemannian optimal identification method for linear continuous-time symmetric systems

Kazuhiro Sato, Hiroyuki Sato, and Tobias Damm

Abstract—This study develops identification methods for linear continuous-time symmetric systems, such as electrical network systems, multi-agent network systems, and temperature dynamics in buildings. To this end, we formulate three system identification problems for the corresponding discrete-time systems. The first is a least-squares problem in which we wish to minimize the sum of squared errors between the true and model outputs on the product manifold of the manifold of symmetric positive-definite matrices and two Euclidean spaces. In the second problem, to reduce the search dimensions, the product manifold is replaced with the quotient set under a specified group action by the orthogonal group. In the third problem, the manifold of symmetric positive-definite matrices in the first problem is replaced by the manifold of matrices with only positive diagonal elements. In particular, we examine the quotient geometry in the second problem. We propose Riemannian conjugate gradient methods for the three problems, and select initial points using a popular subspace method. The effectiveness of our proposed methods is demonstrated through numerical simulations and comparisons with the Gauss–Newton method, which is one of the most popular approach for solving least-squares problems.

Index Terms—Riemannian optimization, symmetry, system identification

I. INTRODUCTION

MANY important systems involved in electrical networks [1]–[3], multi-agent networks [4], [5], and temperature dynamics in buildings [6], [7] can be modeled as

$$\begin{cases} \dot{\hat{x}}(t) = F\hat{x}(t) + G\hat{u}(t), \\ \hat{y}(t) = H\hat{x}(t), \end{cases} \quad (1)$$

where $\hat{x}(t) \in \mathbf{R}^n$, $\hat{u}(t) \in \mathbf{R}^m$, and $\hat{y}(t) \in \mathbf{R}^p$ are the state, input, and output of the system, respectively, and $F \in \text{Sym}(n)$, $G \in \mathbf{R}^{n \times m}$, and $H \in \mathbf{R}^{p \times n}$ are constant matrices. Because the matrix F is symmetric, we call (1) a linear continuous-time symmetric system. In controlling a system described by (1), it is important to have an accurate identification of (F, G, H) .

However, no identification methods for system (1) have yet been developed. More specifically, although many identification techniques have been developed for discrete-time systems, such as prediction error methods [8]–[13] and subspace identification methods [14]–[20] for discrete-time systems, as well as for continuous-time systems [21]–[26], it is difficult to

identify a symmetric matrix F from the $K+1$ input/output data $\{(u_0, y_0), (u_1, y_1), \dots, (u_K, y_K)\}$ over the sampling interval h . Here, y_0, y_1, \dots, y_K are noisy data observed from the true system, which is different from (1). This is because no system identification method has been derived for the corresponding discrete-time system

$$\begin{cases} \hat{x}_{k+1} = A\hat{x}_k + B\hat{u}_k, \\ \hat{y}_k = C\hat{x}_k, \end{cases} \quad (2)$$

where $\hat{x}_k := \hat{x}(kh)$, $\hat{u}_k := \hat{u}(kh)$, $\hat{y}_k := \hat{y}(kh)$, and

$$A := \exp(Fh) \in \text{Sym}_+(n), \quad (3)$$

$$B := \left(\int_0^h \exp(Ft) dt \right) G, \quad (4)$$

$$C := H. \quad (5)$$

That is, the existing methods in [8]–[20] for identifying the triplet (A, B, C) do not provide a symmetric positive-definite matrix A .

For this reason, we present novel prediction error methods for identifying

$$\Theta := (A, B, C) \in M := \text{Sym}_+(n) \times \mathbf{R}^{n \times m} \times \mathbf{R}^{p \times n}$$

using the input/output data $\{(u_0, y_0), (u_1, y_1), \dots, (u_K, y_K)\}$ under the assumption that the matrix A is stable. That is, we identify the matrix A to be symmetric positive definite. If this is achieved, we can also obtain the matrices F , G , and H by

$$F = \log A/h, \quad (6)$$

$$G = \left(\int_0^h \exp(Ft) dt \right)^{-1} B, \quad (7)$$

$$H = C. \quad (8)$$

In particular, the matrix F is symmetric and is uniquely determined, because the map $\exp : \text{Sym}(n) \rightarrow \text{Sym}_+(n)$ is bijective [27].

To develop the prediction error methods, we formalize three different problems by introducing the Riemannian metric

$$\begin{aligned} & \langle (\xi_1, \eta_1, \zeta_1), (\xi_2, \eta_2, \zeta_2) \rangle_\Theta \\ & := \text{tr}(A^{-1}\xi_1 A^{-1}\xi_2) + \text{tr}(\eta_1^\top \eta_2) + \text{tr}(\zeta_1^\top \zeta_2) \end{aligned} \quad (9)$$

for $(\xi_1, \eta_1, \zeta_1), (\xi_2, \eta_2, \zeta_2) \in T_\Theta M$, where the metric has also been used for a model reduction problem [28]. The first problem is the least-squares problem of minimizing the sum of squared errors on the Riemannian manifold M . In the second problem, to reduce the search dimension of the first problem, the manifold M is replaced by the quotient set $M/O(n)$ under

K. Sato is with the Division of Information and Communication Engineering, Kitami Institute of Technology, Hokkaido 090-8507, Japan, email: ksato@mail.kitami-it.ac.jp

H. Sato is with the Department of Applied Mathematics, Graduate School of Informatics, Kyoto University, Kyoto 606-8501, Japan, email: hsato@amp.i.kyoto-u.ac.jp

T. Damm is with the Department of Mathematics, University of Kaiserslautern, Kaiserslautern, Germany, email: damm@mathematik.uni-kl.de

a specific group action of the orthogonal group $O(n)$. In the third problem, we replace the $\text{Sym}_+(n)$ component of M with $\text{Diag}_+(n)$.

The contributions of this paper are summarized as follows.

1) In Section III-C, we show that although, to the best of our knowledge, it is an open problem whether the quotient set $M/O(n)$ in the second problem is a manifold, the set $N/O(n)$ is indeed a manifold, where

$$N := M \cap S_{\text{con}} \cap S_{\text{ob}}. \quad (10)$$

Here,

$$\begin{aligned} S_{\text{con}} &:= \{(A, B, C) \in \mathbf{R}^{n \times n} \times \mathbf{R}^{n \times m} \times \mathbf{R}^{p \times n} \mid \\ &\quad (A, B, C) \text{ is controllable}\}, \\ S_{\text{ob}} &:= \{(A, B, C) \in \mathbf{R}^{n \times n} \times \mathbf{R}^{n \times m} \times \mathbf{R}^{p \times n} \mid \\ &\quad (A, B, C) \text{ is observable}\}, \end{aligned}$$

where we say that (A, B, C) is controllable (resp. observable) if the corresponding discrete-time system described by (2) is controllable (resp. observable). Moreover, in Section III-C1, we prove that Riemannian metric (9) on M induces a Riemannian metric into $N/O(n)$ by using a general theorem, as shown in Appendix C. That is, the quotient set $N/O(n)$ is shown to be a Riemannian manifold.

2) In Section IV, we propose Riemannian conjugate gradient (CG) methods for solving the aforementioned three problems. In developing the CG method for the first problem, we derive the Riemannian gradient of the objective function in terms of Riemannian metric (9), and use the concept of parallel transport. For the modified second problem on the quotient manifold $N/O(n)$, the parallel transport in the first problem is replaced by the projection onto the horizontal space that is a subspace of a tangent space of the manifold N , although the Riemannian gradient is the same. In Section III-C2, it is shown that the projection is obtained using the skew-symmetric solution to a linear matrix equation. In Appendix E, we prove that there exists a unique skew-symmetric solution to the equation under a mild assumption. Moreover, for the third problem, we derive another Riemannian gradient different from that in the first and second problems. Furthermore, in Section IV-D, we propose a technique for choosing initial points in the proposed algorithms for solving the three problems based on a subspace method such as N4SID [17], MOESP [19], CVA [15], ORT [14], or N2SID [20].

3) We demonstrate the effectiveness of our proposed methods for single-input single-output (SISO) and multi-input multi-output (MIMO) cases:

- Our proposed methods for solving the aforementioned three problems can produce $A \in \text{Sym}_+(n)$, unlike the Gauss–Newton (GN) method, which has been widely used for solving least-squares problems. In other words, we illustrate that the usual GN method as explained in Section V is not adequate for identifying system (1).
- Our proposed methods significantly improve the results produced by a modified MOESP method in terms of various indices.
- In MIMO cases, the rate of instability in the estimated matrix A_{est} produced by our method when solving the

third problem is much higher than that for solving the first and second problems. In other words, the proposed methods for solving the first and second problems have a high degree of stability.

- A hybrid approach combining the CG methods for solving the first and second problems may be more efficient than the individual CG methods.

The remainder of this paper is organized as follows. In Section II, we formulate the aforementioned three problems mathematically. In Section III, we discuss Riemannian geometries of our problems. In particular, in Section III-C, we show that the quotient set $N/O(n)$ is a manifold. Moreover, we prove that Riemannian metric (9) on M induces a Riemannian metric on $N/O(n)$ in Section III-C1. In Section IV, we propose optimization algorithms for solving the three problems. In addition, we propose a technique for choosing an initial point in the algorithms. In Section V, we summarize the GN method. In Section VI, we demonstrate the effectiveness of our proposed methods. Finally, the conclusions of this study are presented in Section VII.

Notation: The sets of real and complex numbers are denoted by \mathbf{R} and \mathbf{C} , respectively. The symbols $\text{Sym}(n)$ and $\text{Skew}(n)$ denote the vector spaces of symmetric matrices and skew-symmetric matrices in $\mathbf{R}^{n \times n}$, respectively. The symbol $\text{Diag}(n)$ is the vector space of diagonal matrices in $\mathbf{R}^{n \times n}$. The manifold of symmetric positive definite matrices in $\text{Sym}(n)$ is denoted by $\text{Sym}_+(n)$. The manifold of matrices with positive diagonal elements in $\text{Diag}(n)$ is denoted by $\text{Diag}_+(n)$. The symbol $O(n)$ denotes the orthogonal group in $\mathbf{R}^{n \times n}$. The tangent space at p on a manifold M is denoted by $T_p M$. The identity matrix of size n is denoted by I_n . Given vectors $v = (v_i), w = (w_i) \in \mathbf{R}^n$, (v, w) denotes the Euclidean inner product, i.e.,

$$(v, w) = \sum_{i=1}^n v_i w_i,$$

and $\|v\|_2$ denotes the Euclidean norm, i.e.,

$$\|v\|_2 := \sqrt{(v, v)} = \sqrt{v_1^2 + v_2^2 + \cdots + v_n^2}.$$

Given a matrix $A \in \mathbf{R}^{n \times n}$, $\|A\|_F$ denotes the Frobenius norm, i.e.,

$$\|A\|_F := \sqrt{\text{tr}(A^\top A)},$$

where the superscript \top denotes the transpose and $\text{tr}(A)$ denotes the trace of A , i.e., the sum of the diagonal elements of A . The symbol $\lambda(A)$ denotes the set of eigenvalues of A , and $\text{sym}(A)$ and $\text{sk}(A)$ denote the symmetric and skew-symmetric parts of A , respectively, i.e., $\text{sym}(A) = \frac{A+A^\top}{2}$ and $\text{sk}(A) = \frac{A-A^\top}{2}$. For any matrices $A \in \mathbf{R}^{n \times m}$ and $B \in \mathbf{R}^{p \times q}$, $A \otimes B$ denotes the Kronecker product of A and B , i.e.,

$$A \otimes B := \begin{pmatrix} a_{11}B & a_{12}B & \cdots & a_{1m}B \\ a_{21}B & a_{22}B & \cdots & a_{2m}B \\ \vdots & \vdots & \ddots & \vdots \\ a_{n1}B & a_{n2}B & \cdots & a_{nm}B \end{pmatrix} \in \mathbf{R}^{np \times mq}.$$

Given a smooth function f between finite dimensional normed spaces \mathcal{E} and \mathcal{F} , the Fréchet derivative $Df(x) : \mathcal{E} \rightarrow \mathcal{F}$ of f at $x \in \mathcal{E}$ is defined as a linear operator such that

$$\lim_{\xi \rightarrow 0} \frac{\|f(x + \xi) - f(x) - Df(x)[\xi]\|_{\mathcal{F}}}{\|\xi\|_{\mathcal{E}}} = 0,$$

where $Df(x)[\xi]$ is called the directional derivative of f at x in the direction ξ , and $\|\cdot\|_{\mathcal{E}}$ and $\|\cdot\|_{\mathcal{F}}$ are norms on \mathcal{E} and \mathcal{F} , respectively.

II. PROBLEM SETTINGS

This section presents the formulation of the three problems.

As described earlier, the aim of this study is to develop a novel prediction error method for identifying $\Theta \in M$ using the input/output data. To this end, we consider the following problem.

Problem 1: Suppose that the input/output data $\{(u_0, y_0), (u_1, y_1), \dots, (u_K, y_K)\}$ and state dimension n are given. Then, find the minimizer of

$$\begin{aligned} &\text{minimize} \quad f_1(\Theta) := \|e(\Theta)\|_2^2 \\ &\text{subject to} \quad \Theta \in M. \end{aligned}$$

Here,

$$e(\Theta) := \begin{pmatrix} y_1 - \hat{y}_1(\Theta) \\ y_2 - \hat{y}_2(\Theta) \\ \vdots \\ y_K - \hat{y}_K(\Theta) \end{pmatrix} \in \mathbf{R}^{pK}, \quad (11)$$

and $\hat{y}_k(\Theta)$ is \hat{y}_k obtained by substituting the input data u_k into \hat{u}_k of (2). The initial state $\hat{x}_0 \in \mathbf{R}^n$ in (2) is free. Note that $\hat{y}_k(\Theta)$ is different from the output data y_k , which is obtained by observing the output of the true system. That is, (2) is a mathematical model, but is not the true system.

It is possible to reduce the dimension of the problem of minimizing $\|e(\Theta)\|_2^2$ under the assumption that the initial state \hat{x}_0 is equal to zero. This is because Θ and

$$U \circ \Theta := (U^\top A U, U^\top B, C U)$$

realize input/output equivalent systems for any $U \in O(n)$, where \circ denotes a group action of $O(n)$ on M . That is, they attain the same value of the prediction error, i.e., $\|e(\Theta)\|_2 = \|e(U \circ \Theta)\|_2$. Moreover, if $\Theta \in M$, $U \circ \Theta \in M$ for any $U \in O(n)$. This leads to the idea of equating Θ with $U \circ \Theta$ to reduce the dimension of the problem of minimizing $\|e(\Theta)\|_2^2$.

To this end, we endow M with an equivalence relation \sim , where $\Theta_1 \sim \Theta_2$ if and only if there exists some $U \in O(n)$ such that $\Theta_2 = U \circ \Theta_1$. Defining the equivalence class $[\Theta]$ by $[\Theta] := \{\Theta_1 \in M | \Theta_1 \sim \Theta\}$, we can equate Θ with any Θ_1 that is equivalent to Θ . Thus, instead of Problem 1, we consider the following.

Problem 2: Suppose that the input/output data $\{(u_0, y_0), (u_1, y_1), \dots, (u_K, y_K)\}$ and state dimension n are given. Then, find the minimizer of

$$\begin{aligned} &\text{minimize} \quad f_2([\Theta]) := \|e(\Theta)\|_2^2 \\ &\text{subject to} \quad [\Theta] \in M/O(n) := \{[\Theta] | \Theta \in M\}. \end{aligned}$$

That is, we also develop a prediction error method on the quotient set $M/O(n)$. Note that this development is different from that in [12], which considered a group action of the general linear group $GL(n)$ on a manifold instead of that of $O(n)$. It is not adequate to use the action in [12] for our problem, because this action does not, in general, preserve the symmetric positive-definiteness of the matrix A . For this reason, we consider the group action of $O(n)$ on the manifold M .

Moreover, we can consider a simpler problem than Problems 1 and 2. This is because, for any $\Theta \in M$, there is some $\tilde{U} \in O(n)$ such that

$$\tilde{U} \circ \Theta = (\Lambda, \tilde{U}^\top B, C \tilde{U}),$$

where $\Lambda \in \text{Diag}_+(n)$. That is, the above Θ and $\tilde{U} \circ \Theta$ realize input/output equivalent systems, i.e., $\|e(\Theta)\|_2 = \|e(\tilde{U} \circ \Theta)\|_2$, under the assumption that the initial state \hat{x}_0 is equal to zero. The simpler problem is formulated as follows.

Problem 3: Suppose that the input/output data $\{(u_0, y_0), (u_1, y_1), \dots, (u_K, y_K)\}$ and state dimension n are given. Then, find the minimizer of

$$\begin{aligned} &\text{minimize} \quad f_3(\Theta) := \|e(\Theta)\|_2^2 \\ &\text{subject to} \quad \Theta \in \tilde{M}. \end{aligned}$$

Here, $\tilde{M} := \text{Diag}_+(n) \times \mathbf{R}^{n \times m} \times \mathbf{R}^{p \times n}$. However, we demonstrate in Section VI that, if the output data y_0, y_1, \dots, y_K are noisy, the results provided by our algorithm for solving Problem 3 are more noise sensitive than those produced by our algorithms for solving Problems 1 and 2.

Remark 1: In this paper, we assume that the state dimension n is given. In practice, the dimension n must be determined before solving Problems 1, 2, and 3. For example, we can determine n by using Akaike's information criterion [29] or calculating the singular value decomposition of a matrix related to the input and output matrices [30].

Remark 2: As mentioned in Section I, we can identify (F, G, H) in (1) using (6), (7) and (8) after the identification of (A, B, C) in (2). In addition to Problems 1, 2, and 3, we consider the following problem.

$$\begin{aligned} &\text{minimize} \quad \|\exp(Fh) - A\|_F^2 \\ &\text{subject to} \quad F \in \text{Sym}(n). \end{aligned}$$

One may think that, by solving the above problem, $F \in \text{Sym}(n)$ for (1) can be obtained even if $A \notin \text{Sym}_+(n)$. However, this is not true. For example, if $A = \begin{pmatrix} 0 & 0 \\ 0 & 1 \end{pmatrix}$,

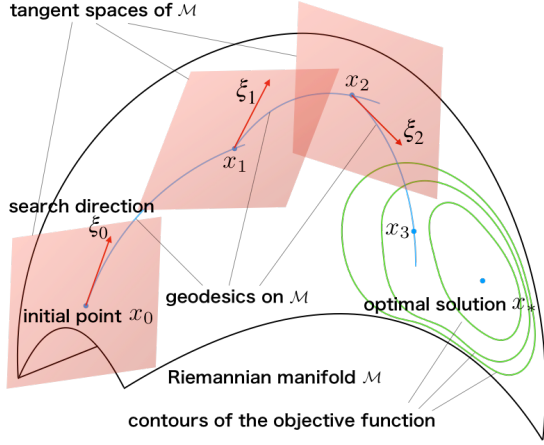


Fig. 1. Optimization process on a Riemannian manifold \mathcal{M} .

then there is no solution F to the above problem. In fact, the infimum of the objective function is 0, whereas this value cannot be obtained with any $F \in \text{Sym}(n)$.

Remark 3: Note that system (1) does not correspond to a symmetric continuous-time system discussed in [3], [31]. Here, system (1) is said to be symmetric in the sense of the definition in [3], [31] if there exists some $T \in GL(n) \cap \text{Sym}(n)$ such that $F^\top T = TF$ and $H^\top = TG$.

III. GEOMETRIES OF PROBLEMS 1, 2, AND 3

A. Riemannian optimization

In preparation for subsequent subsections, we introduce the concepts of the exponential mapping and the Riemannian gradient for Riemannian optimization [32]–[34], and provide a brief description of the optimization algorithm. In this subsection, we consider a general Riemannian optimization problem of minimizing an objective function f defined on a Riemannian manifold \mathcal{M} . That is, \mathcal{M} is equipped with a Riemannian metric $\langle \cdot, \cdot \rangle$ that endows the tangent space $T_x \mathcal{M}$ at each point $x \in \mathcal{M}$ with an inner product.

Fig. 1 illustrates an optimization process on \mathcal{M} . As shown in this figure, the next point is determined by using geodesics and search direction vectors. The following explains the details.

1) *Exponential mapping:* For the purpose of optimization on a Riemannian manifold \mathcal{M} , the update formula $x + \xi$ does not make sense for $x \in \mathcal{M}$ and $\xi \in T_x \mathcal{M}$. This is in contrast to the case of optimization on a Euclidean space \mathcal{E} . That is, on \mathcal{E} , we can compute a point $x_+ \in \mathcal{E}$ from the current point $x \in \mathcal{E}$ and search direction $d \in \mathcal{E}$ as $x_+ = x + d$. Thus, we seek the next point x_+ on a curve called a geodesic on \mathcal{M} emanating from x in the direction of ξ . For any $x, y \in \mathcal{M}$, on a geodesic between two points x and y that are sufficiently close, the path along the geodesic is the shortest among all curves connecting x and y . It is known that, for any $\xi \in T_x \mathcal{M}$, there exists an interval $I \subset \mathbb{R}$ around 0 and a unique geodesic $\Gamma_{(x, \xi)} : I \rightarrow \mathcal{M}$ such that $\Gamma_{(x, \xi)}(0) = x$ and $\dot{\Gamma}_{(x, \xi)}(0) = \xi$. The exponential mapping Exp at $x \in \mathcal{M}$ can be defined through the geodesic as

$$\text{Exp}_x(\xi) := \Gamma_{(x, \xi)}(1),$$

because the geodesic $\Gamma_{(x, \xi)}$ has the homogeneity property $\Gamma_{(x, a\xi)}(t) = \Gamma_{(x, \xi)}(at)$ for any $a \in \mathbb{R}$ satisfying $at \in I$.

2) *Riemannian gradient:* In addition to the exponential mapping, we need a Riemannian gradient to solve our problems. The Riemannian gradient $\text{grad } f(x)$ of f at $x \in \mathcal{M}$ is defined as a tangent vector at x that satisfies

$$Df(x)[\xi] = \langle \text{grad } f(x), \xi \rangle_x$$

for any $\xi \in T_x \mathcal{M}$, where $Df(x) : T_x \mathcal{M} \rightarrow \mathbb{R}$ is a linear mapping called the derivative of f at x , and $Df(x)[\xi]$ is defined as

$$Df(x)[\xi] := (\xi f)(x).$$

Note that a tangent vector can be identified with a derivative.

3) *Algorithm:* The update formula of a gradient algorithm for minimizing the objective function f on \mathcal{M} is given by

$$x_{k+1} = \text{Exp}_{x_k}(\xi_k)$$

with an initial point $x_0 \in \mathcal{M}$, where $\xi_k \in T_{x_k} \mathcal{M}$ is a search direction defined by using the Riemannian gradients.

B. Geometry of Problem 1

In first-order optimization algorithms such as the steepest descent and conjugate gradient methods on the manifold M , we need the Riemannian gradient of the objective function f_1 . To this end, we must introduce a Riemannian metric into M . In this paper, we define the Riemannian metric (9).

Let \tilde{f}_1 denote the extension of the objective function f_1 to the ambient Euclidean space $\mathbb{R}^{n \times n} \times \mathbb{R}^{n \times m} \times \mathbb{R}^{p \times n}$. Then, the directional derivative of \tilde{f}_1 at $\Theta \in M$ along $\xi = (\xi_A, \xi_B, \xi_C) \in T_\Theta M$ is given by

$$D\tilde{f}_1(\Theta)[\xi] = 2(\text{De}(\Theta)[\xi], e(\theta)), \quad (12)$$

where

$$\text{De}(\Theta)[\xi] = \begin{pmatrix} -D\hat{y}_1(\Theta)[\xi] \\ -D\hat{y}_2(\Theta)[\xi] \\ \vdots \\ -D\hat{y}_K(\Theta)[\xi] \end{pmatrix}. \quad (13)$$

Eq. (2) implies that

$$D\hat{y}_k(\Theta)[\xi] = C \sum_{i=0}^{k-1} A^{k-i-1} (\xi_A \hat{x}_i + \xi_B u_i) + \xi_C \hat{x}_k. \quad (14)$$

It follows from (12), (13), and (14) that

$$D\tilde{f}_1(\Theta)[\xi] = \text{tr}(\xi_A \text{sym}(G_A)) + \text{tr}(\xi_B^\top G_B) + \text{tr}(\xi_C^\top G_C), \quad (15)$$

where

$$G_A := -2 \sum_{k=1}^K \sum_{i=0}^{k-1} A^{k-i-1} C^\top (y_k - \hat{y}_k(\Theta)) \hat{x}_i^\top, \quad (16)$$

$$G_B := -2 \sum_{k=1}^K \sum_{i=0}^{k-1} A^{k-i-1} C^\top (y_k - \hat{y}_k(\Theta)) u_i^\top, \quad (17)$$

$$G_C := -2 \sum_{k=1}^K (y_k - \hat{y}_k(\Theta)) \hat{x}_k^\top. \quad (18)$$

Here, we used the property $\xi_A = \xi_A^\top$. Thus, the Euclidean gradient of \bar{f}_1 at Θ is given by

$$\nabla \bar{f}_1(\Theta) = (G_A, G_B, G_C). \quad (19)$$

In [12], we can find a similar derivation for a more complicated system. Because we introduced Riemannian metric (9), the Euclidean gradient in (19) yields the Riemannian gradient

$$\text{grad } f_1(\Theta) = (A \text{sym}(G_A)A, G_B, G_C). \quad (20)$$

For a detailed explanation, see Appendix A.

C. Geometry of Problem 2

It is an open problem whether the quotient set $M/O(n)$ is a manifold, although this set is a Hausdorff space from Proposition 21.4 in [35]. In fact, although there are topological studies on control systems [36]–[40], there is no existing work on the quotient set $M/O(n)$. Thus, it is difficult to guarantee that $\pi^{-1}([\Theta])$ is a submanifold of M for all $\Theta \in M$, because we cannot use well-known results such as Proposition 3.4.4 in [32]. Here, the map $\pi : M \rightarrow M/O(n)$ denotes the canonical projection, i.e., $\pi(\Theta) = [\Theta]$ for any $\Theta \in M$. If $\pi^{-1}([\Theta])$ is not a manifold for some $\Theta \in M$, then $T_\Theta \pi^{-1}([\Theta])$ cannot be defined. That is, in this case, we cannot consider the vertical space in $T_\Theta M$. As a result, it may be impossible to define the horizontal space that is the orthogonal complement of the vertical space with respect to metric (9). This makes it difficult to develop a Riemannian conjugate gradient method for solving Problem 2.

To resolve this issue, we consider the set N defined by (10) instead of M . The set N is an open submanifold of $\mathbf{R}^{n \times n} \times \mathbf{R}^{p \times m} \times \mathbf{R}^{p \times n}$, because, in addition to M , S_{con} and S_{ob} are open sets in $\mathbf{R}^{n \times n} \times \mathbf{R}^{n \times m} \times \mathbf{R}^{p \times n}$, as shown in Proposition 3.3.12 in [41]. A group action of $O(n)$ on N , as in M , is given by

$$U \circ \Theta := (U^\top A U, U^\top B, C U), \quad (21)$$

where $\Theta \in N$. Then, $U \circ \Theta \in N$ for any $U \in O(n)$. By introducing the equivalence class $[\Theta] := \{\Theta_1 \in N \mid \Theta_1 \sim \Theta\}$, we can define the quotient set $N/O(n) := \{[\Theta] \mid \Theta \in N\}$.

Unlike $M/O(n)$, we can guarantee that $N/O(n)$ is a manifold using the quotient manifold theorem [35], which is explained in Appendix B. To see this, we must confirm that action (21) is free and proper. Action (21) is proper because the Lie group $O(n)$ is compact. For a more detailed explanation, see Corollary 21.6 in [35]. Thus, we show that action (21) is free. Suppose that the general linear group $GL(n)$ acts on N as

$$T \diamond \Theta := (T^{-1} A T, T^{-1} B, C T), \quad T \in GL(n), \Theta \in N.$$

This action is free, as explained in Remark 6.5.10 in [41]. That is,

$$\{T \in GL(n) \mid T \diamond \Theta = \Theta\} = \{I_n\} \quad (22)$$

for any $\Theta \in N$. Moreover, we have that

$$\{I_n\} \subset \{U \in O(n) \mid U \circ \Theta = \Theta\} \subset \{T \in GL(n) \mid T \diamond \Theta = \Theta\} \quad (23)$$

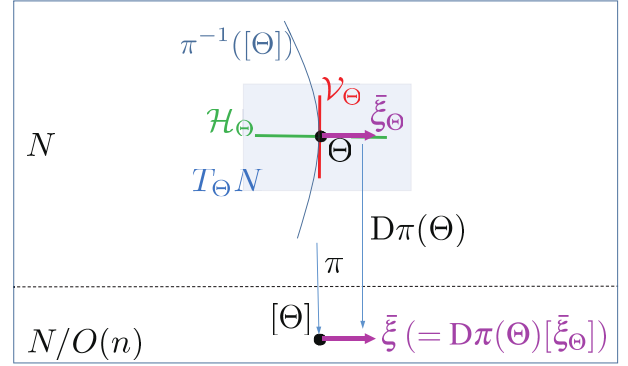


Fig. 2. Conceptual diagram of vertical space \mathcal{V}_Θ , horizontal space \mathcal{H}_Θ , and horizontal lift $\bar{\xi}_\Theta$.

for any $\Theta \in N$. From (22) and (23), action (21) is free.

Because $N/O(n)$ is a quotient manifold, Proposition 3.4.4 in [32] implies that $\pi^{-1}([\Theta])$ is an embedded submanifold of N for any $\Theta \in N$. Thus, we can define the vertical space $\mathcal{V}_\Theta := T_\Theta \pi^{-1}([\Theta])$ in $T_\Theta N$ for any $\Theta \in N$. Moreover, from Proposition 3.9 in [35], $T_\Theta M = T_\Theta N$ for any $\Theta \in N$, because N is an open set in M . Hence, we can consider \mathcal{V}_Θ in $T_\Theta M$ for any $\Theta \in N \subset M$. Additionally, the horizontal space \mathcal{H}_Θ can be defined as the orthogonal complement of the vertical space \mathcal{V}_Θ in $T_\Theta N$ with respect to metric (9). Furthermore, the horizontal lift $\bar{\xi}_\Theta \in \mathcal{H}_\Theta$ of $\xi \in T_{[\Theta]}(N/O(n))$ is defined as the unique element of the horizontal space \mathcal{H}_Θ satisfying $D\pi(\Theta)[\bar{\xi}_\Theta] = \xi$. Fig. 2 presents a diagram of these concepts.

1) *Riemannian metric on the quotient manifold $N/O(n)$:* In the following, we show that a Riemannian metric on $N/O(n)$ can be defined by

$$\langle \xi, \zeta \rangle_{[\Theta]} := \langle \bar{\xi}_\Theta, \bar{\zeta}_\Theta \rangle_\Theta, \quad (24)$$

where $\xi, \zeta \in T_{[\Theta]}(N/O(n))$, $\Theta \in \pi^{-1}([\Theta])$, and $\bar{\xi}_\Theta$ and $\bar{\zeta}_\Theta$ are the horizontal lifts of ξ and ζ at $\Theta \in N$, respectively. Note that $\langle \cdot, \cdot \rangle_\Theta$ of the right-hand side of (24) is Riemannian metric (9).

To this end, we must prove that

$$\langle \bar{\xi}_{\Theta_1}, \bar{\zeta}_{\Theta_1} \rangle_{\Theta_1} = \langle \bar{\xi}_{\Theta_2}, \bar{\zeta}_{\Theta_2} \rangle_{\Theta_2} \quad (25)$$

for any $\Theta_1, \Theta_2 \in \pi^{-1}([\Theta])$. To prove this, we first note that (9) yields

$$\langle D\phi_U(\Theta)[\xi_1], D\phi_U(\Theta)[\xi_2] \rangle_{\phi_U(\Theta)} = \langle \xi_1, \xi_2 \rangle_\Theta \quad (26)$$

for any $\xi_1, \xi_2 \in T_\Theta N$ and any $U \in O(n)$, where $\phi_U(\Theta) := U \circ \Theta$. That is, the group action ϕ_U is an isometry in terms of Riemannian metric (9). Eq. (26) implies the following theorem.

Theorem 1: For any $U \in O(n)$,

$$\bar{\xi}_{\phi_U(\Theta)} = D\phi_U(\Theta)[\bar{\xi}_\Theta]. \quad (27)$$

We provide the proof of Theorem 1 in Appendix C.

Using Theorem 1 and (26), we can prove (25) as follows: For any $\Theta_1, \Theta_2 \in \pi^{-1}([\Theta])$, there exists some $U \in O(n)$ such that $\Theta_2 = \phi_U(\Theta_1)$. Thus,

$$\begin{aligned} \langle \bar{\xi}_{\Theta_2}, \bar{\zeta}_{\Theta_2} \rangle_{\Theta_2} &= \langle \bar{\xi}_{\phi_U(\Theta_1)}, \bar{\zeta}_{\phi_U(\Theta_1)} \rangle_{\phi_U(\Theta_1)} \\ &= \langle D\phi_U(\Theta_1)[\bar{\xi}_{\Theta_1}], D\phi_U(\Theta_1)[\bar{\zeta}_{\Theta_1}] \rangle_{\phi_U(\Theta_1)} \\ &= \langle \bar{\xi}_{\Theta_1}, \bar{\zeta}_{\Theta_1} \rangle_{\Theta_1}, \end{aligned}$$

where the second and third equalities follow from (27) and (26), respectively.

Note that (25) is based on isometric condition (26) in terms of Riemannian metric (9). In other words, if (26) is not satisfied, we cannot conclude that (25) holds.

2) *Orthogonal projection onto the horizontal space \mathcal{H}_Θ* : In Section IV-B, we need the concept of vector transport (which is a generalized concept of parallel transport [32]) on $N/O(n)$ to develop a Riemannian conjugate gradient method. To this end, for any $\Theta \in N$, we use the orthogonal projection P_Θ onto the horizontal space \mathcal{H}_Θ .

To derive P_Θ , we need to explicitly describe the vertical space \mathcal{V}_Θ and the horizontal space \mathcal{H}_Θ . First, we specify \mathcal{V}_Θ . Consider any curve $\Theta(t)$ on $\pi^{-1}([\Theta]) \subset N$ with $\Theta(0) = \Theta$ that is expressed as

$$\Theta(t) = (U^\top(t)AU(t), U^\top(t)B, CU(t)),$$

where $U(t)$ denotes a curve on $O(n)$ with $U(0) = I_n$. Differentiating both sides with respect to t , we obtain

$$\dot{\Theta}(0) = (\dot{U}^\top(0)A + A\dot{U}(0), \dot{U}^\top(0)B, C\dot{U}(0)),$$

where $\dot{U}(0) \in T_{I_n}O(n) \cong \text{Skew}(n)$. Thus, we have that

$$\mathcal{V}_\Theta = \{(-U'A + AU', -U'B, CU') \mid U' \in \text{Skew}(n)\}.$$

Next, we characterize the horizontal space \mathcal{H}_Θ . Let $(A', B', C') \in \mathcal{H}_\Theta$. That is,

$$\langle (-U'A + AU', -U'B, CU'), (A', B', C') \rangle_\Theta = 0 \quad (28)$$

for all $U' \in \text{Skew}(n)$. This means that

$$\text{tr}(U'(2A'A^{-1} + BB'^\top + C^\top C')) = 0.$$

Because $U' \in \text{Skew}(n)$ is arbitrary, we conclude that

$$2A'A^{-1} + BB'^\top + C^\top C' \in \text{Sym}(n).$$

That is,

$$\text{sk}(2A'A^{-1} + BB'^\top + C^\top C') = 0.$$

Thus,

$$\mathcal{H}_\Theta \subset \{(A', B', C') \mid \text{sk}(2A'A^{-1} + BB'^\top + C^\top C') = 0\}.$$

Conversely, if $(A', B', C') \in \{(A', B', C') \mid \text{sk}(2A'A^{-1} + BB'^\top + C^\top C') = 0\}$, we have that $(A', B', C') \in \mathcal{H}_\Theta$, because (28) holds. Hence, we obtain

$$\mathcal{H}_\Theta = \{(A', B', C') \mid \text{sk}(2A'A^{-1} + BB'^\top + C^\top C') = 0\}. \quad (29)$$

We are in a position to describe the orthogonal projection P_Θ onto the horizontal space \mathcal{H}_Θ .

Theorem 2: The orthogonal projection P_Θ onto \mathcal{H}_Θ is given by

$$P_\Theta(\eta) = \eta + (XA - AX, XB, -CX), \quad (30)$$

where $\eta = (a, b, c) \in T_\Theta N$, and X is the skew-symmetric solution to the linear matrix equation

$$\mathcal{L}_1(X) + 2\mathcal{L}_0(X) + \beta = 0, \quad (31)$$

where the linear matrix mappings $\mathcal{L}_0, \mathcal{L}_1 : \mathbf{R}^{n \times n} \rightarrow \mathbf{R}^{n \times n}$ are defined by

$$\begin{aligned} \mathcal{L}_0(X) &:= AXA^{-1} + A^{-1}XA - 2X, \\ \mathcal{L}_1(X) &:= (BB^\top + C^\top C)X + X(BB^\top + C^\top C), \end{aligned}$$

and $\beta := 2\text{sk}(2A^{-1}a + bB^\top + c^\top C)$.

We provide the proof in Appendix D.

We can guarantee that there exists a unique solution $X \in \text{Skew}(n)$ to (31) under the assumption

$$\dim(\text{Ker}(\lambda I_n - A) \cap \text{Ker} B^\top \cap \text{Ker} C) \leq 1 \quad \text{for any } \lambda \in \mathbf{R}. \quad (32)$$

Assumption (32) holds if matrix A has only simple eigenvalues, because then $\dim(\text{Ker}(\lambda I_n - A)) \leq 1$ for all $\lambda \in \mathbf{R}$. Furthermore, if (A, C) is observable, i.e.,

$$\text{rank} \begin{pmatrix} \lambda I_n - A \\ C \end{pmatrix} = n \Leftrightarrow \text{Ker}(\lambda I_n - A) \cap \text{Ker} C = \{0\}$$

for all $\lambda \in \mathbf{C}$, then (32) holds. Analogously, the controllability of (A, B) , i.e.,

$$\text{rank} \begin{pmatrix} \lambda I_n - A & B \end{pmatrix} = \text{rank} \begin{pmatrix} \lambda I_n - A \\ B^\top \end{pmatrix} = n,$$

also implies (32).

Theorem 3: Assume that (32) holds, and let $\mathcal{L} := \mathcal{L}_1 + 2\mathcal{L}_0$. Then, $\text{Ker} \mathcal{L} = \text{Ker} \mathcal{L}_1 \cap \text{Ker} \mathcal{L}_0 \subset \text{Ker} \mathcal{L}_0 \subset \text{Sym}(n)$. In particular, $\mathcal{L} : \text{Skew}(n) \rightarrow \text{Skew}(n)$ is an automorphism. That is, for any $Y \in \text{Skew}(n)$, there exists a unique $X \in \text{Skew}(n)$ with $\mathcal{L}(X) = Y$.

The proof is given in Appendix E.

3) *Riemannian gradient*: In numerical computations, we can use the horizontal lift $\overline{\text{grad}} f_{2\Theta}$ as the Riemannian gradient at $[\Theta] \in N/O(n)$. The horizontal lift belongs to the horizontal space \mathcal{H}_Θ , and we have that

$$\overline{\text{grad}} f_{2\Theta} = \text{grad} f_1(\Theta), \quad (33)$$

as shown in Section 3.6.2 in [32]. Thus, as the Riemannian gradient at $[\Theta] \in N/O(n)$, we can use $\text{grad} f_1(\Theta)$, i.e., (20).

D. Geometry of Problem 3

Similarly to Riemannian metric (9) on M , we define the Riemannian metric on \tilde{M} as

$$\begin{aligned} &\langle (\xi_1, \eta_1, \zeta_1), (\xi_2, \eta_2, \zeta_2) \rangle_\Theta \\ &:= \text{tr}(A^{-1}\xi_1 A^{-1}\xi_2) + \text{tr}(\eta_1^\top \eta_2) + \text{tr}(\zeta_1^\top \zeta_2) \\ &= \text{tr}((A^{-1})^2 \xi_1 \xi_2) + \text{tr}(\eta_1^\top \eta_2) + \text{tr}(\zeta_1^\top \zeta_2) \end{aligned} \quad (34)$$

for $(\xi_1, \eta_1, \zeta_1), (\xi_2, \eta_2, \zeta_2) \in T_\Theta \tilde{M}$. Here, the second equality follows from the fact that A^{-1} , ξ_1 , and ξ_2 are diagonal matrices.

Let \bar{f}_3 denote the extension of the objective function f_3 to the ambient Euclidean space $\mathbf{R}^{n \times n} \times \mathbf{R}^{n \times m} \times \mathbf{R}^{p \times n}$. Then, the directional derivative of \bar{f}_3 at $\Theta \in \tilde{M}$ along $\xi = (\xi_A, \xi_B, \xi_C) \in T_\Theta \tilde{M}$ is given by

$$\begin{aligned} D\bar{f}_3(\Theta)[\xi] &= \text{tr}(\xi_A^\top G_A) + \text{tr}(\xi_B^\top G_B) + \text{tr}(\xi_C^\top G_C) \\ &= \text{tr}(\xi_A \text{diag}(G_A)) + \text{tr}(\xi_B^\top G_B) + \text{tr}(\xi_C^\top G_C), \end{aligned} \quad (35)$$

where G_A , G_B , and G_C are defined by (16), (17), and (18), respectively. Here, we used the property that $\xi_A \in T_A \text{Diag}_+(n) \cong \text{Diag}(n)$. Moreover, it follows from (42) and $Df_3(\Theta)[\xi] = \langle \text{grad } f_3(\Theta), \xi \rangle_\Theta$ that

$$Df_3(\Theta)[\xi] = \text{tr}((A^{-1})^2(\text{grad } f_3(\Theta))_A \xi_A) + \text{tr}(\xi_B^\top (\text{grad } f_3(\Theta))_B) + \text{tr}(\xi_C^\top (\text{grad } f_3(\Theta))_C). \quad (36)$$

Because $Df_3(\Theta)[\xi] = D\bar{f}_3(\Theta)[\xi]$, (35) and (36) yield

$$\text{grad } f_3(\Theta) = (A^2 \text{diag}(G_A), G_B, G_C).$$

IV. OPTIMIZATION ALGORITHMS FOR SOLVING PROBLEMS 1, 2, AND 3

This section describes optimization algorithms for solving Problems 1, 2, and 3, and introduces a technique for choosing initial points in the algorithms.

A. Optimization algorithm for solving Problem 1

Algorithm 1 describes a Riemannian CG method for solving Problem 1. Because the Riemannian metric on the manifold M is defined by (9), the exponential map Exp on M is given by

$$\begin{aligned} \text{Exp}_\Theta(A', B', C') &= (A^{1/2} \exp(A^{-1/2} A' A^{-1/2}) A^{1/2}, B + B', C + C') \\ &= (A \exp(A^{-1} A'), B + B', C + C'), \end{aligned} \quad (37)$$

and the parallel transport \mathcal{P} is given by

$$\begin{aligned} \mathcal{P}_{\Theta_1, \Theta_2}(A', B', C') &= ((A_2 A_1^{-1})^{1/2} A' ((A_2 A_1^{-1})^{1/2})^\top, B', C'), \end{aligned} \quad (38)$$

where $\Theta_i = (A_i, B_i, C_i) \in M$ ($i = 1, 2$), as shown in [42]. We choose t_k in step 4 as the Armijo step size [32]. The parameter β_{k+1} in step 5 is called the Dai–Yuan type parameter [43].

The computational complexity of calculating the gradient $\text{grad } f_1(\Theta)$ is higher than that of the other steps in Algorithm 1. To estimate the complexity, we examine the complexities of G_A , G_B and G_C . To this end, we note that G_A in (16) can be rewritten as

$$G_A = -2 \sum_{i=0}^{K-1} \sum_{k=i+1}^K A^{k-i-1} C^\top (y_k - \hat{y}_k(\Theta)) \hat{x}_i^\top.$$

Thus, we can recursively calculate G_A as

$$G_A(i+1) = G_A(i) - 2\gamma(i) \hat{x}_{K-(i+1)}^\top, \quad (39)$$

where

$$\begin{aligned} G_A(0) &= 0, \\ \gamma(i) &= C^\top (y_{K-i} - \hat{y}_{K-i}(\Theta)) + A\gamma(i-1), \\ \gamma(0) &= C^\top (y_K - \hat{y}_K(\Theta)). \end{aligned}$$

In fact, $G_A(K) = G_A$. If $p < n$, i.e., the number of outputs is less than that of states, the computational complexity of $\gamma(i) \hat{x}_{K-(i+1)}^\top$ for each $i \in \{0, 1, \dots, K-1\}$ in (39) is $\mathcal{O}(n^2)$, because that of $\gamma(i)$ for each $i \in \{0, 1, \dots, K-1\}$ is $\mathcal{O}(n^2)$.

Thus, the complexity of G_A is $\mathcal{O}(Kn^2)$. Similarly, if $m < n$ and $p < n$, then the complexity of G_B is $\mathcal{O}(Kn^2)$. Moreover, if $p < n$, (18) implies that the complexity of G_C is $\mathcal{O}(Kn^2)$. Hence, if $p, m < n < K$, (20) implies that the complexity of $\text{grad } f_1(\Theta)$ is $\mathcal{O}(Kn^2)$.

Algorithm 1 Optimization algorithm for solving Problem 1.

- 1: Set input/output data $\{(u_0, y_0), (u_1, y_1), \dots, (u_K, y_K)\}$, the state dimension n , and an initial point $\Theta_0 := (A_0, B_0, C_0) \in M$.
- 2: Set $\eta_0 = -\text{grad } f_1(\Theta_0)$ using (20).
- 3: **for** $k = 0, 1, 2, \dots$ **do**
- 4: Compute a step size $t_k > 0$, and set

$$\Theta_{k+1} = \text{Exp}_{\Theta_k}(t_k \eta_k). \quad (40)$$

- 5: Set

$$\beta_{k+1} = \frac{\|g_{k+1}\|_{k+1}^2}{\langle g_{k+1}, \mathcal{P}_{\Theta_k, \Theta_{k+1}}(\eta_k) \rangle_{k+1} - \langle g_k, \eta_k \rangle_k},$$

where $g_k := \text{grad } f_1(\Theta_k)$, and $\|\cdot\|_k$ and $\langle \cdot, \cdot \rangle_k$ denote the norm and the inner product in the tangent space $T_{\Theta_k} M$, respectively.

- 6: Set

$$\eta_{k+1} = -g_{k+1} + \beta_{k+1} \mathcal{P}_{\Theta_k, \Theta_{k+1}}(\eta_k). \quad (41)$$

- 7: **end for**
-

B. Optimization algorithm for solving Problem 2

To develop a practical algorithm for solving Problem 2 based on the Riemannian CG method, we regard the set $M/O(n)$ as the quotient manifold $N/O(n)$. We believe this is natural, because Proposition 3.3.12 in [41] implies that the manifold N is a dense set in the manifold M . The proposed CG-based method is obtained by replacing the parallel transport $\mathcal{P}_{\Theta_k, \Theta_{k+1}}$ in Algorithm 1 with the orthogonal projection $P_{\Theta_{k+1}}$ given by (30) onto the horizontal space $\mathcal{H}_{\Theta_{k+1}}$. The orthogonal projection $P_{\Theta_{k+1}}$ is a vector transport on the quotient manifold $N/O(n)$ [32].

C. Optimization algorithm for solving Problem 3

The Riemannian CG method for solving Problem 3 is the same as Algorithm 1, except for the following:

- Replace M with \tilde{M} .
- Replace $\text{grad } f_1(\Theta_k)$ with $\text{grad } f_3(\Theta_k)$.

However, the computational complexity is lower than in the case of Problem 1. This is because the matrices A_k ($k = 0, 1, \dots$) in Algorithm 1 are diagonal when solving Problem 3, unlike for Problem 1.

D. Initial points in Algorithm 1

To select an initial point $\Theta_0 \in M$ in Algorithm 1 for solving Problems 1 and 2, we propose Algorithm 2 in which rand denotes a single uniformly distributed random number in the interval $(0, 1)$. In step 1, we obtain a triplet (A, B, C) using an

existing subspace method such as N4SID [17], MOESP [19], CVA [15], ORT [14], or N2SID [20]. However, at this stage, A is not contained in $\text{Sym}_+(n)$, but also $A \notin \text{Sym}(n)$. Thus, in step 2, we replace A with the symmetric part of A . That is, at this stage, $A \in \text{Sym}(n)$, but $A \notin \text{Sym}_+(n)$ in general. In fact, if there is $i \in \{1, 2, \dots, n\}$ such that $\lambda_i \leq 0$ in step 3, $A \notin \text{Sym}_+(n)$. In steps 4, 5, \dots , 8, any negative eigenvalues of A are replaced with a random value in $(0, 0.01)$. That is, we consider negative eigenvalues of A to be perturbations of small positive eigenvalues. Thus, steps 9 and 10 produce $A \in \text{Sym}_+(n)$ and $\Theta_0 \in M$, respectively.

For Problem 3, we replace step 9 in Algorithm 2 with

$$A \leftarrow \text{diag}(\lambda_1, \lambda_2, \dots, \lambda_n), \quad B \leftarrow V^\top B, \quad C \leftarrow CV,$$

where $V := (v_1 \ v_2 \ \dots \ v_n)$. Then, Θ_0 in step 10 is contained in \hat{M} .

Algorithm 2 Constructing the initial point $\Theta_0 \in M$.

- 1: Set (A, B, C) using a subspace method.
 - 2: $A \leftarrow \text{sym}(A)$.
 - 3: Let $A = \sum_{i=1}^n \lambda_i v_i v_i^\top$ be the eigenvalue decomposition. That is, λ_i is an eigenvalue of A , and v_i is the associated eigenvector.
 - 4: **for** $i = 1, 2, \dots, n$ **do**
 - 5: **if** $\lambda_i \leq 0$ **then**
 - 6: $\lambda_i = 0.01 \times \text{rand}$.
 - 7: **end if**
 - 8: **end for**
 - 9: $A \leftarrow \sum_{i=1}^n \lambda_i v_i v_i^\top$.
 - 10: $\Theta_0 := (A, B, C)$.
-

Remark 4: A Riemannian steepest descent (SD) method for solving Problems 1 and 2 can be derived by replacing steps 5 and 6 in Algorithm 1 with $\eta_{k+1} = -\text{grad } f_1(\Theta_{k+1})$. That is, in contrast to the case of the CG methods, the SD method for Problem 2 is the same as that for Problem 1, because (33) holds. However, the SD method is not more efficient than CG methods [44]. We demonstrate this fact in Section VI-A.

Remark 5: Instead of Riemannian metric (9), we can introduce the Riemannian metric

$$\begin{aligned} & \langle (\xi_1, \eta_1, \zeta_1), (\xi_2, \eta_2, \zeta_2) \rangle_\Theta \\ &:= \text{tr}(\xi_1 \xi_2) + \text{tr}(\eta_1^\top \eta_2) + \text{tr}(\zeta_1^\top \zeta_2) \end{aligned} \quad (42)$$

for $(\xi_1, \eta_1, \zeta_1), (\xi_2, \eta_2, \zeta_2) \in T_\Theta M$. Even if we define metric (42) into M , a Riemannian metric on $N/O(n)$ can be defined by (24), because (25) holds under metric (42). However, in this case, the exponential mapping (37) is replaced with

$$\text{Exp}_\Theta(A', B', C') = (A + A', B + B', C + C').$$

Thus, $\text{Exp}_\Theta(A', B', C') \notin M$ for some $(A', B', C') \in T_\Theta M$ because $A + A'$ is not positive-definite. As a result, we have to carefully choose $(A', B', C') \in T_\Theta M$ unlike for Riemannian metric (9).

V. GN METHOD FOR SOLVING OUR PROBLEMS

The GN method has been widely used for solving least-squares problems. Before comparing our proposed methods with the GN method, this section summarizes the GN method.

In the GN method [10], [13], we often use the vector parameter

$$\theta := \begin{pmatrix} \text{vec}_{\text{sym}}(A) \\ \text{vec}(B) \\ \text{vec}(C) \end{pmatrix} \in \mathbf{R}^{n_\theta} \quad (43)$$

with

$$n_\theta := n \left(\frac{n+1}{2} + m + p \right),$$

where vec denotes the usual vec-operator, i.e., $\text{vec}(A) \in \mathbf{R}^{n^2}$ is obtained by stacking the columns of $A \in \mathbf{R}^{n \times n}$, and for a symmetric matrix $A \in \text{Sym}(n)$, $\text{vec}_{\text{sym}}(A)$ denotes the $\frac{1}{2}n(n+1)$ -vector that is obtained from $\text{vec}(A)$ by eliminating the redundant elements. For example, if $A \in \text{Sym}(3)$,

$$\begin{aligned} & \text{vec}(A) \\ &= (a_{11} \ a_{21} \ a_{31} \ a_{12} \ a_{22} \ a_{32} \ a_{13} \ a_{23} \ a_{33})^\top, \\ & \text{vec}_{\text{sym}}(A) \\ &= (a_{11} \ a_{21} \ a_{31} \ a_{22} \ a_{32} \ a_{33})^\top. \end{aligned}$$

The parameter θ defined by (43) is a global coordinate system for the manifold M , and thus we regard Θ on M as θ . Hence, we write the prediction error vector $e(\Theta)$ defined by (11) as $e(\theta)$ and the objective function $f_1(\Theta)$ as

$$V(\theta) := \|e(\theta)\|_2^2.$$

The aim of the GN method is to minimize $V(\theta)$.

The update formula of the GN method is given by

$$\theta_{k+1} = \theta_k + t_k \Delta \theta_k, \quad (44)$$

where $t_k > 0$ is a step size, and $\Delta \theta_k$ satisfies

$$J(\theta_k)^\top J(\theta_k) \Delta \theta_k = -J(\theta_k)^\top e(\theta_k) \quad (45)$$

with

$$J(\theta) := \frac{\partial e}{\partial \theta}(\theta) \in \mathbf{R}^{pK \times n_\theta}. \quad (46)$$

Here,

$$\frac{\partial e}{\partial \theta_i}(\theta) = - \begin{pmatrix} \frac{\partial \hat{y}_1}{\partial \theta_i}(\theta) \\ \frac{\partial \hat{y}_2}{\partial \theta_i}(\theta) \\ \vdots \\ \frac{\partial \hat{y}_K}{\partial \theta_i}(\theta) \end{pmatrix},$$

and

$$\begin{cases} \frac{\partial \hat{y}_j}{\partial \theta_i}(\theta) = \frac{\partial C}{\partial \theta_i} \hat{x}_j + C \frac{\partial \hat{x}_j}{\partial \theta_i}, \\ \frac{\partial \hat{x}_j}{\partial \theta_i} = \frac{\partial A}{\partial \theta_i} \hat{x}_{j-1} + A \frac{\partial \hat{x}_{j-1}}{\partial \theta_i} + \frac{\partial B}{\partial \theta_i} u_{j-1} \end{cases}$$

with $\frac{\partial \hat{x}_0}{\partial \theta_i} = 0$. Note that if $\theta_k \in N \subset M$ and the step size t_k is sufficiently small, then $\Delta \theta_k$ can be regarded as an element of $T_{\theta_k} N$. In this case,

$$e(\theta_k + t_k \Delta \theta_k) \approx e(\theta_k) + t_k J(\theta_k) \Delta \theta_k, \quad (47)$$

and

$$J(\theta_k) : T_{\theta_k} N \rightarrow \mathbf{R}^{pK}. \quad (48)$$

Note that (43) is an overparameterization. This means that different θ may have the equivalent input-output properties. In fact, from Section III-C, each element (A, B, C) of $\pi^{-1}([\Theta]) \subset N$, which can be regarded as different θ , has the same input-output properties, where the dimension of $\pi^{-1}([\Theta])$ is

$$\dim \pi^{-1}([\Theta]) = \dim N - \dim N/O(n) = \frac{n(n-1)}{2}. \quad (49)$$

Eq. (49) follows from Proposition 1 in Appendix B and Proposition 3.4.4 in [32]. Hence, if $\Delta\theta_k \in T_{\theta_k} \pi^{-1}([\Theta_k]) \subset T_{\theta_k} N$ under the identification of Θ_k and θ_k , it follows from (47) that $J(\theta_k) \Delta\theta_k = 0$, that is, $\Delta\theta_k \in \text{Ker } J(\theta_k)$. Therefore,

$$T_{\theta_k} \pi^{-1}([\Theta_k]) \subset \text{Ker } J(\theta_k),$$

and (49) yields

$$\dim \text{Ker } J(\theta_k) \geq \frac{n(n-1)}{2}. \quad (50)$$

It follows from (50) that the matrix $J(\theta_k)$ is rank deficient, and thus there are infinitely many solutions to (45). In the data-driven local coordinates (DDLC) introduced in [10], $\Delta\theta_k$ is chosen as

$$\Delta\theta_k = -V_1 S_1^{-1} U_1^\top e(\theta_k) \quad (51)$$

as shown in [13], where $U_1 S_1 V_1^\top$ is the truncated singular value decomposition of $J(\theta_k)$, and $S_1 \in \mathbf{R}^{n_\theta \times n_\theta}$ is a diagonal matrix.

Remark 6: Although the Jacobian $J(\theta)$ is rank-deficient in our case, if $J(\theta)$ is of full-rank, update formula (44) for the GN method can be regarded as a Riemannian steepest descent method for the specific choice of the Riemannian metric

$$g_\theta^{\text{GN}}(\dot{\theta}_1, \dot{\theta}_2) := \dot{\theta}_1^\top R(\theta) \dot{\theta}_2 \quad (52)$$

with $R(\theta) := 2J(\theta)^\top J(\theta)$ into \mathbf{R}^{n_θ} , as stated in [8], [11]. The Riemannian gradient of the objective function V at $\theta \in \mathbf{R}^{n_\theta}$ is given by

$$R(\theta)^{-1} \frac{\partial V}{\partial \theta}(\theta),$$

where the gradient is called the natural gradient in the Riemannian manifold \mathbf{R}^{n_θ} endowed with the Riemannian metric (52) [45]. Using the natural gradient, update formula (44) can be expressed as

$$\theta_{k+1} = \theta_k - R(\theta_k)^{-1} \frac{\partial V}{\partial \theta}(\theta_k). \quad (53)$$

Remark 7: Update formula (44) preserves the symmetry of A , but does not, in general, preserve the positive-definiteness. More precisely, if θ_k is contained in the manifold M or N , θ_{k+1} given by (44) is also contained in M or N by choosing sufficiently small $t_k > 0$. This is because M and N are open sets. However, if $t_k > 0$ is too small, the objective function V does not change very much. Thus, we need to choose sufficiently large $t_k > 0$, but then θ_{k+1} is not contained in M and N , as demonstrated in Section VI. That is, it is difficult to determine an appropriate step size t_k for some examples.

Remark 8: Instead of using the full parameterization $\theta \in \mathbf{R}^{n_\theta}$ defined by (43), we can use canonical forms of linear

systems, which reduce the number of free parameters. However, canonical forms may lead to numerically ill-conditioned problems due to noise, as pointed out in Sections 1 and 4 in [10]. Moreover, the results of Section VI-B1 justify this point, because Problem 3 can be regarded as a case of using a canonical form. Thus, in practice, the use of canonical forms for system identification may not be adequate.

Remark 9: To resolve the numerically ill-conditioned problem as mentioned in Remark 8, the use of overlapping parameterization has been proposed in [46], and the authors in [39] introduced block-balanced input normal forms, which are overlapping parameterizations. However, this approach requires monitoring the condition of the parametrization and switching to a new structure if the current structure is bad. That is, this needs a number of extra calculations, which are not necessary in the case of Algorithm 1 based on Riemannian optimization.

VI. NUMERICAL SIMULATIONS

In this section, we demonstrate the effectiveness of the proposed method. To this end, we evaluate the identified systems using various indices, in addition to the value of the objective function in Problems 1, 2, and 3, to prevent overfitting to noisy data. Note that, in the simulations, we used MOESP [19] as the subspace method for step 1 in Algorithm 2. This was implemented in the *system identification toolbox* of MATLAB. Hence, we can easily implement Algorithm 2.

We consider identification problems of the RC electrical network system [1], [2] represented as the undirected graph $\mathcal{G} = \{\{1, 2, \dots, n\}, \mathcal{E}\}$, which is composed of n nodes and the set \mathcal{E} of k undirected edges. A mathematical model of the system is described by

$$\begin{cases} C_{\text{cap}} \dot{V}(t) = -(\mathcal{L}_{\text{res}} + G_{\text{con}})V(t) + \tilde{G}u(t), \\ y(t) = \tilde{H}V(t). \end{cases} \quad (54)$$

Table I explains the parameters of system (54). Here, $\mathcal{L}_{\text{res}} := \mathcal{B} R_{\text{res}}^{-1} \mathcal{B}^\top$ is a symmetric positive semi-definite matrix, $\mathcal{B} \in \mathbf{R}^{n \times k}$ is the incidence matrix of \mathcal{G} , and $R_{\text{res}} \in \text{Diag}_+(n)$ is the resistance matrix. The incidence matrix $\mathcal{B} = (\mathcal{B}_{ij}) \in \mathbf{R}^{n \times k}$ is defined by

$$\mathcal{B}_{ij} := \begin{cases} 1, & \text{if } i \text{ is the source node of edge } j \\ -1, & \text{if } i \text{ is the sink node of edge } j \\ 0, & \text{otherwise.} \end{cases}$$

System (54) can be transformed into (1) by defining $x(t) := C_{\text{cap}}^{1/2} V(t)$:

$$\begin{cases} \dot{x}(t) = Fx(t) + Gu(t), \\ y(t) = Hx(t) \end{cases} \quad (55)$$

with

$$\begin{aligned} F &:= -C_{\text{cap}}^{-1/2} (\mathcal{L}_{\text{res}} + G_{\text{con}}) C_{\text{cap}}^{-1/2} \in \mathbf{R}^{n \times n}, \\ G &:= C_{\text{cap}}^{-1/2} \tilde{G} \in \mathbf{R}^{n \times m}, \\ H &:= \tilde{H} C_{\text{cap}}^{1/2} \in \mathbf{R}^{p \times n}. \end{aligned}$$

Note that the matrix $-F$ is contained in $\text{Sym}_+(n)$, and thus F is stable. That is, all the eigenvalues of F are negative.

TABLE I
PARAMETERS OF SYSTEM (54).

$V(t) \in \mathbf{R}^n$	node-voltage vector
$u(t) \in \mathbf{R}^m$	voltage-source vector
$y(t) \in \mathbf{R}^p$	measurement output vector
$C_{\text{cap}} \in \text{Sym}_+(n)$	capacitance matrix
$G_{\text{con}} \in \text{Sym}_+(n)$	conductance matrix
$\mathcal{L}_{\text{res}} \in \text{Sym}(n)$	Laplacian matrix associated with \mathcal{G}
$\tilde{G} \in \mathbf{R}^{n \times m}$ and $\tilde{H} \in \mathbf{R}^{p \times n}$	constant matrices

Although we consider mathematical model (55) to be noise free, measurement noise is inevitable in practice, as explained in Section 4.3 in [9]. Thus, we assume that the true system is given by

$$\begin{cases} x_{k+1} = Ax_k + Bu_k, \\ y_k = Cx_k + v_k, \end{cases} \quad (56)$$

where A , B , and C are defined by (3), (4), and (5), respectively, and $v_k \in \mathbf{R}^p$ is measurement noise. That is, the input/output data (u_k, y_k) is generated by (56). Because F is stable, the matrix A is also stable. That is, all eigenvalues of A are in the interval $(0, 1)$. The signal-to-noise ratio of system (56) is defined as

$$\text{SNR} = 10 \log_{10} \left(\frac{\sum_{k=0}^K \|y_k - v_k\|_2^2}{\sum_{k=0}^K \|v_k\|_2^2} \right). \quad (57)$$

In the following, we present the results of numerical simulations for SISO and MIMO cases. For SISO cases, we illustrate a frequency response using the Bode plots. For MIMO cases, the values of various indices are given, because Bode plots of MIMO cases do not clarify the distance between the true and estimated systems.

To this end, we set $n = 20$, and generated the undirected graph \mathcal{G} using the Watts and Strogatz model [47] with 20 nodes of mean degree 10 and rewiring probability 0.4. Additionally, C_{cap} , R_{res} , and G_{con} were given by

$$\begin{cases} C_{\text{cap}} = 10 \times \text{diag}(\text{rand}, \text{rand}, \dots, \text{rand}), \\ R_{\text{res}} = 0.1 \times \text{diag}(1, 1, \dots, 1), \\ G_{\text{con}} = \text{diag}(\text{rand}, \text{rand}, \dots, \text{rand}), \end{cases} \quad (58)$$

where each rand denotes a uniformly distributed random number in the interval $(0, 1)$. Moreover, we generated each component of u_k from the Gaussian random distribution with mean 0 and variance 100, and the components of v_k from the Gaussian random distribution with mean 0 and variance σ^2 . The sampling interval h was 0.1.

We denote the results given by Algorithm 1 for solving Problems 1, 2, and 3 as CG_1 , CG_2 , and CG_3 , respectively. Moreover, we write SD to denote the Riemannian SD method, as briefly explained in Remark 4.

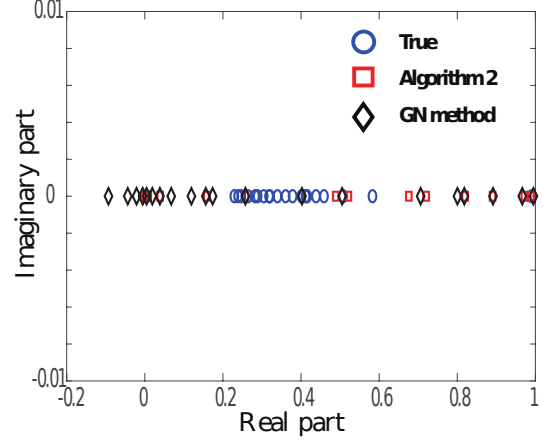


Fig. 3. Eigenvalues of A in the original system, estimated system produced by Algorithm 2, and estimated system provided by the GN method after 10 iterations.

A. SISO case

First, we considered SISO cases with $m = p = 1$. The parameters \tilde{G} and \tilde{H} were given by

$$\tilde{G} = \begin{pmatrix} 1 \\ 0 \\ \vdots \\ 0 \end{pmatrix}, \quad \tilde{H} = (1 \quad 0 \quad \dots \quad 0).$$

1) *Identification by the GN method:* Fig.3 illustrates the eigenvalues of the true matrix A corresponding to F of system (55), the estimated matrix A produced by Algorithm 2, and the estimated matrix A provided by the prediction error method using the GN method with the update formula (44) and (51), as explained in Section V, after 10 iterations. Here, we used the result (A, B, C) obtained by Algorithm 2 as the initial point of the GN method, and the step sizes t_k in (44) were $t_k = 10^{-9}$ for all $k \in \{1, 2, \dots, 10\}$. According to Fig.3, the prediction error method using the GN method did not provide $\Theta \in M$. In fact, some eigenvalues of A produced by the GN method took negative values, whereas all eigenvalues of the true matrix A are positive. Moreover, we confirmed the following results:

- When $t_k = 10^{-9}$, the positive-definite property of matrix A produced by the GN method was lost after only a few iterations.
- If we set $t_k > 10^{-9}$, the symmetric matrices A produced by the GN method, in many cases, were unstable after 10 iterations.
- Even if we set $t_k < 10^{-9}$, some eigenvalues of the symmetric matrices A produced by the GN method were negative after 10 iterations.

Thus, the GN method described in Section V is not adequate for solving our problem. Hence, we hereafter compare CG_1 , CG_2 , CG_3 , SD, and Algorithm 2.

2) *Comparison of CG_1 , CG_2 , CG_3 , and SD:* Figs.4 and 5 illustrate a comparison of CG_1 , CG_2 , CG_3 , and SD with $K = 600$, $\sigma^2 = 0.1$, and $\text{SNR} = 12.803$. Here, Θ_0 in Fig.4 was obtained using Algorithm 2. According to these figures, the results for CG_1 and CG_2 completely overlap, and Fig.4

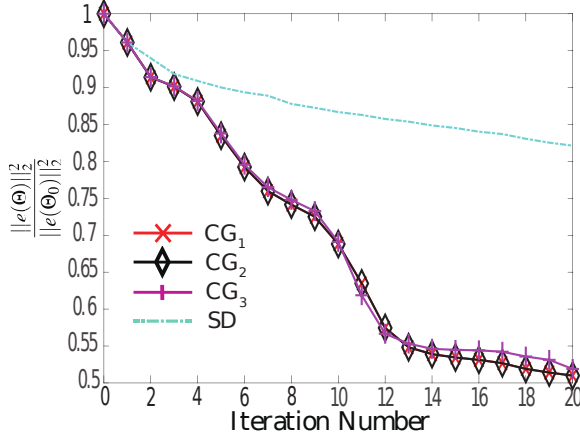


Fig. 4. Relative objective values obtained by CG₁, CG₂, CG₃, and SD.

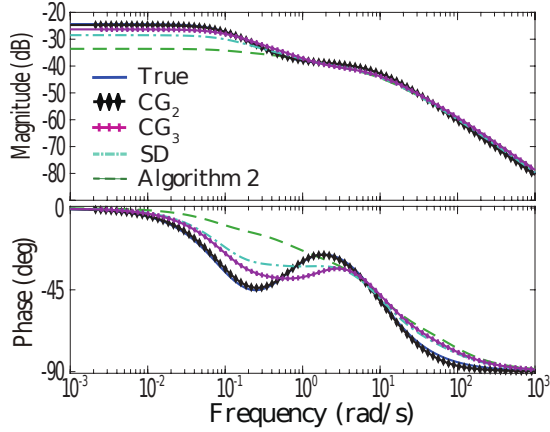


Fig. 5. Bode plots of true and estimated systems obtained by CG₁, CG₂, CG₃, SD, and Algorithm 2.

demonstrates that the convergence speeds of CG₁, CG₂, and CG₃ are superior to that of SD. Moreover, Fig. 5 shows that CG₁, CG₂, CG₃, and SD improve the frequency response of Algorithm 2. In particular, the Bode plots of the estimated systems obtained by CG₁ and CG₂ are almost the same as that of the true system, unlike CG₃, SD, and Algorithm 2.

B. MIMO case

Next, we considered the MIMO case with $m = p = 2$. The parameters \tilde{G} and \tilde{H} were given by

$$\tilde{G} = \begin{pmatrix} 1 & 0 \\ 0 & 1 \\ 0 & 0 \\ \vdots & \vdots \\ 0 & 0 \end{pmatrix}, \quad \tilde{H} = \begin{pmatrix} 1 & 0 & 0 & \cdots & 0 \\ 0 & 1 & 0 & \cdots & 0 \end{pmatrix}.$$

As with the SISO case, the conventional GN method did not produce $A_{\text{est}} \in \text{Sym}_+(n)$ and the convergence speeds of CG₁, CG₂, and CG₃ were faster than that of SD. Thus, we present the results of comparisons among CG₁, CG₂, CG₃, and Algorithm 2.

TABLE II
NUMBER OF UNSTABLE CASES OVER 20 ITERATIONS WHEN $K = 400$.

Algorithm	$\sigma^2 = 0.05$	$\sigma^2 = 0.1$	$\sigma^2 = 0.5$
CG ₁	3	2	3
CG ₂	1	1	2
CG ₃	15	17	26

TABLE III
SNR_{ave} AND SNR_{dev} WHEN $K = 400$.

	$\sigma^2 = 0.05$	$\sigma^2 = 0.1$	$\sigma^2 = 0.5$
SNR _{ave}	26.261	20.174	6.212
SNR _{dev}	6.686	6.660	6.686

1) *Stability of the estimated matrices $A \in \text{Sym}_+(n)$ produced by CG₁, CG₂, and CG₃*: Because all of the matrices A_{est} (estimates of A in true system (56)) produced by CG₁, CG₂, and CG₃ are contained in $\text{Sym}_+(n)$, the eigenvalues of A_{est} are positive real numbers, unlike the eigenvalues given by the conventional GN method. However, even if A is stable, A_{est} may be unstable.

Thus, we compared the stability of the estimated matrices A_{est} provided by CG₁, CG₂, and CG₃. We performed numerical simulations 100 times with $\sigma^2 = 0.05$, $\sigma^2 = 0.1$, and $\sigma^2 = 0.5$. Table II presents the number of unstable cases over 20 iterations when $K = 400$. According to Table II, the rate of instability in A_{est} produced by CG₃ is far higher than when using CG₁ or CG₂. Because we used different C_{cap} , R_{res} , and G_{con} for each simulation, the SNR defined by (57) was also different. Table III describes the relation between σ^2 and SNR. Here, SNR_{ave} and SNR_{dev} are the average and standard deviation over 10000 simulations, defined by

$$\text{SNR}_{\text{ave}} := \frac{\sum_{i=1}^{10000} \text{SNR}_i}{10000},$$

$$\text{SNR}_{\text{dev}} := \sqrt{\frac{\sum_{i=1}^{10000} (\text{SNR}_i - \text{SNR}_{\text{ave}})^2}{10000}},$$

where SNR_i denotes SNR in the i -th simulation. According to Table III, SNR_{ave} decreases as σ^2 increases, although the SNR_{dev} values are similar. We also obtained similar results to those described in Tables II and III for different values of K . Hence, we conclude that the rate of instability in A_{est} produced by CG₃ is far higher than those when using CG₁ and CG₂. In addition, the instability rate for CG₁ and CG₂ is independent of SNR, unlike that for CG₃.

The reason for the high instability rate produced by CG₃ is that the noise component of the output directly influences the diagonal matrix A_{est} , i.e., eigenvalues of A_{est} . This is essentially the same phenomenon observed in system identification problems, whereby canonical forms lead to numerically ill-conditioned problems [10]. In contrast, the noise component does not have a significant effect on the eigenvalues of the estimated matrices A_{est} produced by CG₁ and CG₂, because the matrices are not diagonal.

2) *Evaluation of proposed methods:* We evaluated the results with respect to the cost function $\|e(\Theta_{\text{est}})\|_2^2$, the relative H^2 and H^∞ norms, and the maximum eigenvalues $\lambda_{\max}(F_{\text{est}})$ of the estimated matrix F_{est} of F . Here, $\lambda_{\max}(F)$ was -0.086 in all cases. To define the relative H^2 and H^∞ norms, we use T and T_{est} as the transfer functions from the input u to the output y of the true and estimated systems, respectively. That is,

$$T(s) := C(sI_n - F)^{-1}G, \quad s \in \mathbb{C},$$

$$T_{\text{est}}(s) := C_{\text{est}}(sI_n - F_{\text{est}})^{-1}G_{\text{est}},$$

where G_{est} and C_{est} are the estimated matrices of G and C , respectively. Here, we estimate the matrices F_{est} and G_{est} using (6) and (7), respectively. Using T and \hat{T} , we define the following relative H^2 and H^∞ norms:

$$g_2 := \frac{\|T - T_{\text{est}}\|_{H^2}}{\|T\|_{H^2}} \quad \text{and} \quad g_\infty := \frac{\|T - T_{\text{est}}\|_{H^\infty}}{\|T\|_{H^\infty}}.$$

Tables IV, V, VI, VII, and VIII present values of $\|e(\Theta_{\text{est}})\|_2^2$, g_2 , g_∞ , and $\lambda_{\max}(F_{\text{est}})$ for different K , as given by estimating Θ_{est} , F_{est} , G_{est} , and C_{est} using Algorithm 2, CG₁, CG₂, and a combined CG approach called Hybrid CG. Here, the number of iterations of CG₁ and CG₂ was set to 20. Hybrid CG is a combination of CG₁ and CG₂ obtained by applying CG₁ for the first 15 iterations and CG₂ for the next 5 iterations.

According to Tables IV, V, VI, VII, and VIII, the results for $\|e(\Theta_{\text{est}})\|_2^2$, g_2 , g_∞ , and $\lambda_{\max}(F_{\text{est}})$ given by CG₁ and CG₂ are better than those given by Algorithm 2 for all K . The results from CG₁ and CG₂ are almost the same for all K . However, with the exception of $\lambda_{\max}(F_{\text{est}})$, the results from Hybrid CG are superior to those of CG₁ and CG₂. Even when the combination of iterations was changed, the results of Hybrid CG were better than those of CG₁ and CG₂ in many cases. Moreover, we should note that the evaluation results may be worse as the data length K increases.

Remark 10: In Section VI-B1, we showed that the rate of instability in the estimated matrices produced by CG₃ was significantly higher than in those given by CG₁ and CG₂ in the MIMO case. However, in the SISO case, no destabilization occurred for CG₁, CG₂, or CG₃.

Remark 11: In Section VI-B2, we confirmed the maximum eigenvalue $\lambda_{\max}(F_{\text{est}})$, because the transient state $\hat{x}(t)$ in system (1) is dominated by $\lambda_{\max}(F)$ under $\hat{u}(t) = 0$. That is, if $\lambda_{\max}(F)$ and $\lambda_{\max}(F_{\text{est}})$ are closer, we can expect the true and estimated transient states to be more similar.

Remark 12: In terms of the various indices used in Section VI-B2, we confirmed that Algorithm 2 provides a considerably better initial point Θ_0 in Algorithm 1 than randomly choosing $\Theta_0 \in M$.

Remark 13: When we used our proposed methods CG₁, CG₂, and CG₃, the number of iterations was set to 20. Increasing the number of iterations would decrease the value of the objective function $\|e(\Theta_{\text{est}})\|_2^2$. However, other indices such as g_2 , g_∞ , and $\lambda_{\max}(F_{\text{est}})$ may become worse due to overfitting with noisy data.

Remark 14: Our proposed method for solving Problem 2 has been described in Section IV-B. This method, i.e., CG₂,

TABLE IV
EVALUATION RESULTS WHEN $K = 200$ AND SNR = 15.043.

$K = 200$	$\ e(\Theta_{\text{est}})\ _2^2$	g_2	g_∞	$\lambda_{\max}(F_{\text{est}})$
Algorithm 2	23.097	0.660	0.868	-0.138
CG ₁	4.675	0.288	0.328	-0.075
CG ₂	4.662	0.287	0.322	-0.075
Hybrid CG	4.759	0.241	0.258	-0.098

TABLE V
EVALUATION RESULTS WHEN $K = 400$ AND SNR = 15.286.

$K = 400$	$\ e(\Theta_{\text{est}})\ _2^2$	g_2	g_∞	$\lambda_{\max}(F_{\text{est}})$
Algorithm 2	76.360	0.576	0.774	-0.117
CG ₁	5.231	0.124	0.123	-0.064
CG ₂	5.226	0.124	0.122	-0.064
Hybrid CG	4.900	0.111	0.087	-0.065

TABLE VI
EVALUATION RESULTS WHEN $K = 600$ AND SNR = 15.669.

$K = 600$	$\ e(\Theta_{\text{est}})\ _2^2$	g_2	g_∞	$\lambda_{\max}(F_{\text{est}})$
Algorithm 2	75.850	0.624	0.835	-0.258
CG ₁	7.028	0.144	0.218	-0.067
CG ₂	7.025	0.144	0.217	-0.067
Hybrid CG	6.538	0.072	0.052	-0.100

TABLE VII
EVALUATION RESULTS WHEN $K = 800$ AND SNR = 16.714.

$K = 800$	$\ e(\Theta_{\text{est}})\ _2^2$	g_2	g_∞	$\lambda_{\max}(F_{\text{est}})$
Algorithm 2	358.798	0.653	0.868	-0.387
CG ₁	59.391	0.343	0.263	-0.115
CG ₂	59.000	0.343	0.265	-0.115
Hybrid CG	20.623	0.191	0.211	-0.129

TABLE VIII
EVALUATION RESULTS WHEN $K = 1000$ AND SNR = 16.380.

$K = 1000$	$\ e(\Theta_{\text{est}})\ _2^2$	g_2	g_∞	$\lambda_{\max}(F_{\text{est}})$
Algorithm 2	320.573	0.620	0.831	-0.237
CG ₁	17.541	0.141	0.058	-0.082
CG ₂	17.464	0.141	0.057	-0.082
Hybrid CG	12.865	0.094	0.055	-0.093

worked well, even if the true systems to be identified were not controllable and observable. Moreover, CG₂ even worked well when $\Theta_0 \in M$ but $\Theta_0 \notin N$ in Algorithm 1. Thus, although the manifold M should be replaced with the manifold N in theory, as discussed in Section III-C, the method described in Section IV-B works well for solving Problem 1.

VII. CONCLUSION AND FUTURE WORK

We developed identification methods for linear continuous-time symmetric systems using Riemannian optimization. For this, we formulated three least-squares problems of minimizing the sum of squared errors on Riemannian manifolds, and described the geometry of each problem. In particular, we examined the quotient geometry in one problem in depth. We proposed Riemannian CG methods for the three problems, and selected initial points using the modified MOESP method. The

results from a series of numerical simulations demonstrated the effectiveness of our proposed methods with comparisons to the traditional GN method.

The following problems should be addressed in future studies.

- 1) As mentioned in Remark 3, system (1) does not correspond to a symmetric continuous-time system discussed in [3], [31]. To identify such systems, we need to develop a novel method that is fundamentally different from the methods proposed in this paper.
- 2) In Section VI-B2, we confirmed that the results produced by Hybrid CG, a combination of CG₁ and CG₂, were better than those of CG₁ and CG₂ in many cases. It would be interesting to study how the combination of iterations of CG₁ and CG₂ should be determined.
- 3) Lemma 2 in [37] shows that the manifold of transfer functions of SISO systems, i.e., $m = p = 1$, is partitioned into multiple connected components. Thus, it is expected that $N/O(n)$ with $m = p = 1$ will have multiple connected components, because each element in $N/O(n)$ corresponds to a transfer function. If this is the case, different initial points on the different connected components will converge to different points, and thus initial points on $N/O(n)$ may considerably affect the system identification results. In fact, as mentioned in Remark 12, we have confirmed that Algorithm 2 provides a better initial point than a random choice. This provides a practical insight, and so it would be interesting to study whether or not the expectation is true.
- 4) In this paper, we proposed methods for identifying a target system as (1) with no noise. As illustrated in Section VI, our proposed methods are effective for identifying (1), even if the output data was noisy. However, if we were to consider the effect of noise on our methods, we may be able to derive better algorithms. Thus, it is desirable to extend our proposed methods under the consideration of noise.

ACKNOWLEDGMENT

This work was supported by JSPS KAKENHI Grant Numbers JP18K13773 and JP16K17647, and the Asahi Glass Foundation.

APPENDIX

A. Geometry of the manifold $\text{Sym}_+(n)$

We review the geometry of $\text{Sym}_+(n)$ to develop optimization algorithms for solving our problems. For a detailed explanation, see [28], [48].

For $\xi_1, \xi_2 \in T_S \text{Sym}_+(n)$, we define Riemannian metric into $\text{Sym}_+(n)$ as

$$\langle \xi_1, \xi_2 \rangle_S := \text{tr}(S^{-1} \xi_1 S^{-1} \xi_2). \quad (59)$$

Let $f : \text{Sym}_+(n) \rightarrow \mathbf{R}$ be a smooth function and \bar{f} be the extension of f to Euclidean space $\mathbf{R}^{n \times n}$. Riemannian gradient $\text{grad } f(S)$ with respect to Riemannian metric (59) is given by

$$\text{grad } f(S) = S \text{sym}(\nabla \bar{f}(S)) S, \quad (60)$$

where $\nabla \bar{f}(S)$ denotes the Euclidean gradient of \bar{f} at $S \in \text{Sym}_+(n)$. The exponential map on $\text{Sym}_+(n)$ is given by

$$\begin{aligned} \text{Exp}_S(\xi) &= S^{\frac{1}{2}} \exp(S^{-\frac{1}{2}} \xi S^{-\frac{1}{2}}) S^{\frac{1}{2}} \\ &= S \exp(S^{-1} \xi), \end{aligned} \quad (61)$$

where \exp is the matrix exponential function.

We note that Riemannian metric (59) is essentially the same with Fisher information metric

$$g_S^{\text{FIM}} := \mathbf{E}(\text{D}l_x(S) \otimes \text{D}l_x(S)),$$

where

$$l_x(S) := \log p(x|S^{-1}),$$

\mathbf{E} is the expectation operator with respect to $p(x|S^{-1})$, and \otimes is the tensor product. Here, $p(x|S^{-1})$ denotes the Gaussian distribution with zero mean vector and covariance $S^{-1} \in \text{Sym}_+(n)$, that is,

$$p(x|S^{-1}) = \sqrt{\frac{\det S}{(2\pi)^n}} \exp\left(-\frac{1}{2}x^\top S x\right).$$

Thus, $l_x(S)$ is the log-likelihood function of $p(x|S^{-1})$, and

$$l_x(S) = -\frac{n}{2} \log(2\pi) + \frac{1}{2} \log \det S - \frac{1}{2}x^\top S x. \quad (62)$$

To see the relation between (59) and g_S^{FIM} , we use

$$g_S^{\text{FIM}} = -\mathbf{E}(\text{D}^2 l_x(S)), \quad (63)$$

where $\text{D}^2 l_x(S) : \text{Sym}(n) \times \text{Sym}(n) \rightarrow \mathbf{R}$ is the second derivative of l_x at S . Eq. (63) can be found in Theorem 1 in [48]. The directional derivative of $l_x : \text{Sym}(n) \rightarrow \mathbf{R}$ at $S \in \text{Sym}_+(n)$ along $\xi \in T_S \text{Sym}_+(n) \cong \text{Sym}(n)$ is given by

$$\text{D}l_x(S)[\xi] = \frac{1}{2} \text{tr}(S^{-1} \xi) - \frac{1}{2} \text{tr}(x x^\top \xi), \quad (64)$$

where the first term of the right-hand side is obtained by using Jacobi's formula $\text{D} \det S[\xi] = \text{tr}(\det(S) S^{-1} \xi)$. We define the inner product of $\text{Sym}(n)$ as $\text{tr}(\xi_1 \xi_2)$ for any $\xi_1, \xi_2 \in \text{Sym}(n)$. Then, from (64), the gradient of l_x at $S \in \text{Sym}_+(n)$ is provided as

$$\nabla l_x(S) = \frac{1}{2}(S^{-1} - x x^\top).$$

Moreover, according to [32], the Hessian of l_x at S is given by

$$\text{Hess } l_x(S)[\xi] = \text{D} \nabla l_x(S)[\xi] = -\frac{1}{2} S^{-1} \xi S^{-1}, \quad (65)$$

and

$$\text{D}^2 l_x(S)[\xi_1, \xi_2] = \text{tr}(\text{Hess } l_x(S)[\xi_1] \xi_2). \quad (66)$$

Substituting (65) into (66), we obtain that

$$\text{D}^2 l_x(S)[\xi_1, \xi_2] = -\frac{1}{2} \text{tr}(S^{-1} \xi_1 S^{-1} \xi_2). \quad (67)$$

That is, $\text{D}^2 l_x(S)[\xi_1, \xi_2]$ is independent of x . Hence, from (59), (63), and (67), we obtain that

$$g_S^{\text{FIM}}(\xi_1, \xi_2) = -\text{D}^2 l_x(S)[\xi_1, \xi_2] = \frac{1}{2} \langle \xi_1, \xi_2 \rangle_S.$$

Thus, Riemannian metric (59) is essentially the same with Fisher information metric g_S^{FIM} .

B. Quotient manifold theorem

This appendix explains how to use the following quotient manifold theorem as shown in Theorem 21.10 in [35] in our discussion of Section III-C.

Proposition 1: Suppose that \mathcal{G} is a Lie group acting smoothly, freely, and properly on a smooth manifold \mathcal{M} . Then, the orbit space \mathcal{M}/\mathcal{G} is a topological manifold of dimension equal to $\dim \mathcal{M} - \dim \mathcal{G}$, and has a unique smooth structure with the property that the quotient map $\pi : \mathcal{M} \rightarrow \mathcal{M}/\mathcal{G}$ is a smooth submersion.

Here, the action \cdot of Lie group \mathcal{G} on a smooth manifold \mathcal{M} is called

- free if

$$\{g \in \mathcal{G} \mid g \cdot p = p\} = \{e\}$$

for each $p \in \mathcal{M}$, where e is the identity of \mathcal{G} .

- proper if the map $f : \mathcal{G} \times \mathcal{M} \rightarrow \mathcal{M} \times \mathcal{M}$ defined by $(g, p) \mapsto (g \cdot p, p)$ is a proper map. That is, for every compact set $K \in \mathcal{M} \times \mathcal{M}$, the preimage $f^{-1}(K) \subset \mathcal{G} \times \mathcal{M}$ is compact.

We can apply the quotient manifold theorem in our case, if (21) is a free and proper action. This is because the orthogonal group $O(n)$ is a Lie group, and (21) is a smooth action on the smooth manifold N . We thus confirm that action (21) is free and proper in Section III-C.

C. Proof of Theorem 1

In this appendix, we provide the proof of Theorem 1 without deriving specific expressions of the vertical and horizontal spaces. More concretely, we prove a more general theorem, and point out that Theorem 1 is a corollary of the general theorem.

Let \mathcal{M} be a Riemannian manifold with the Riemannian metric $\langle \cdot, \cdot \rangle$, and let \mathcal{G} be a group that smoothly acts on \mathcal{M} . Here, we call $\phi_g : \mathcal{M} \rightarrow \mathcal{M}$ a smooth group action if ϕ_g is smooth and satisfies the following.

- 1) For any $g_1, g_2 \in \mathcal{G}$ and any $x \in \mathcal{M}$, $\phi_{g_1 g_2}(x) = \phi_{g_1}(\phi_{g_2}(x))$ holds.
- 2) For the identity element $1_{\mathcal{G}} \in \mathcal{G}$ and any $x \in \mathcal{M}$, $\phi_{1_{\mathcal{G}}}(x) = x$ holds.

We write the derivative map of ϕ_g at $x \in \mathcal{M}$ as $D\phi_g(x) : T_x \mathcal{M} \rightarrow T_{\phi_g(x)} \mathcal{M}$. By definition,

$$\begin{aligned} D\phi_{1_{\mathcal{G}}}(x) &= D(\phi_{g^{-1}} \circ \phi_g)(x) \\ &= D\phi_{g^{-1}}(\phi_g(x)) \circ D\phi_g(x), \end{aligned}$$

and thus

$$D\phi_{g^{-1}}(\phi_g(x)) = (D\phi_g(x))^{-1}. \quad (68)$$

Let \mathcal{M}/\mathcal{G} be a quotient Riemannian manifold of \mathcal{M} with the canonical projection $\pi : \mathcal{M} \rightarrow \mathcal{M}/\mathcal{G}$. That is, $\pi(x) = [x]$ for any $x \in \mathcal{M}$, where $[x] := \{x_1 \in \mathcal{M} \mid x = \phi_g(x_1) \text{ for some } g \in \mathcal{G}\}$. Let $\mathcal{V}_x := T_x \pi^{-1}([x])$ be the vertical space in $T_x \mathcal{M}$, and let \mathcal{H}_x be the horizontal space that is the orthogonal complement of \mathcal{V}_x with respect to the metric $\langle \cdot, \cdot \rangle$. Let V be a vector space in $T_x \mathcal{M}$, and let

$$D\phi_g(x)[V] := \{D\phi_g(x)[\xi] \mid \xi \in V\}.$$

Lemma 1: For any $g \in \mathcal{G}$ and $x \in \mathcal{M}$,

$$\mathcal{V}_{\phi_g(x)} = D\phi_g(x)[\mathcal{V}_x]. \quad (69)$$

Proof : Let $\xi \in \mathcal{V}_{\phi_g(x)} = T_{\phi_g(x)} \pi^{-1}([\phi_g(x)])$. Then, there exists a curve γ such that $\gamma(0) = \phi_g(x)$ and $\dot{\gamma}(0) = \xi$. Because \mathcal{G} acts on \mathcal{M} , $\gamma_0(t) := \phi_{g^{-1}}(\gamma(t))$ is on $\pi^{-1}([x])$. We have that

$$\gamma_0(0) = \phi_{g^{-1}}(\phi_g(x)) = x,$$

and

$$\dot{\gamma}_0(t) = D\phi_{g^{-1}}(\gamma(t))[\dot{\gamma}(t)].$$

Hence, it follows from (68) that

$$\begin{aligned} \dot{\gamma}_0(0) &= D\phi_{g^{-1}}(\phi_g(x))[\xi] \\ &= (D\phi_g(x))^{-1}[\xi] \in T_x \pi^{-1}([x]) = \mathcal{V}_x, \end{aligned}$$

and thus $\xi \in D\phi_g(x)[\mathcal{V}_x]$. That is,

$$\mathcal{V}_{\phi_g(x)} \subset D\phi_g(x)[\mathcal{V}_x].$$

Considering the dimension of both sides, we obtain (69). \square

Lemma 1 implies the following theorem.

Theorem 4: Suppose that the group action ϕ_g is an isometry in terms of Riemannian metric $\langle \cdot, \cdot \rangle$; i.e., for any $g \in \mathcal{G}$ and any $\xi_1, \xi_2 \in T_x \mathcal{M}$,

$$\langle D\phi_g(x)[\xi_1], D\phi_g(x)[\xi_2] \rangle_{\phi_g(x)} = \langle \xi_1, \xi_2 \rangle_x. \quad (70)$$

Then,

$$\mathcal{H}_{\phi_g(x)} = D\phi_g(x)[\mathcal{H}_x]. \quad (71)$$

Proof : Taking the orthogonal complement of both sides of (69), we have that

$$\mathcal{H}_{\phi_g(x)} = (D\phi_g(x)[\mathcal{V}_x])^\perp. \quad (72)$$

Because (70) holds, we obtain that

$$\langle D\phi_g(x)[\xi_1], D\phi_g(x)[\xi_2] \rangle_{\phi_g(x)} = \langle \xi_1, \xi_2 \rangle_x = 0$$

for any $\xi_1 \in \mathcal{V}_x$ and $\xi_2 \in \mathcal{H}_x$. This means that $D\phi_g(x)[\xi_2] \in (D\phi_g(x)[\mathcal{V}_x])^\perp$, which yields

$$D\phi_g(x)[\mathcal{H}_x] \subset (D\phi_g(x)[\mathcal{V}_x])^\perp.$$

Considering the dimension of both sides, we have that

$$D\phi_g(x)[\mathcal{H}_x] = (D\phi_g(x)[\mathcal{V}_x])^\perp. \quad (73)$$

It follows from (72) and (73) that (71) holds. \square

Theorem 4 yields the following corollary.

Corollary 1: Suppose that the group action ϕ_g is an isometry in terms of Riemannian metric $\langle \cdot, \cdot \rangle$; i.e., (70) holds for any $g \in \mathcal{G}$ and any $\xi_1, \xi_2 \in T_x \mathcal{M}$. Then,

$$\bar{\xi}_{\phi_g(x)} = D\phi_g(x)[\bar{\xi}_x], \quad (74)$$

where $\bar{\xi}_x$ and $\bar{\xi}_{\phi_g(x)}$ are the horizontal lifts of $\xi \in T_{[x]}(\mathcal{M}/\mathcal{G})$ at $x \in \mathcal{M}$ and $\phi_g(x) \in \mathcal{M}$, respectively.

Proof : Because $\pi \circ \phi_g = \pi$,

$$D(\pi \circ \phi_g)(x)[\bar{\xi}_x] = D\pi(x)[\bar{\xi}_x] = \xi, \quad (75)$$

where the second equality follows from the definition of the horizontal lift. Moreover, by the chain rule,

$$D(\pi \circ \phi_g)(x)[\bar{\xi}_x] = D\pi(\phi_g(x))[D\phi_g(x)[\bar{\xi}_x]]. \quad (76)$$

It follows from (75) and (76) that

$$D\pi(\phi_g(x))[D\phi_g(x)[\bar{\xi}_x]] = \xi,$$

and Theorem 4 yields

$$D\phi_g(x)[\bar{\xi}_x] \in \mathcal{H}_{\phi_g(x)}.$$

By the definition of the horizontal lift, we obtain (74). \square

Theorem 1 follows from Corollary 1. This is because the group action $\phi_U(\Theta) := U \circ \Theta$ is an isometry, as shown in (26).

D. Proof of Theorem 2

Because $T_\Theta N = \mathcal{V}_\Theta \oplus \mathcal{H}_\Theta$, η can be uniquely decomposed into

$$\eta = \eta^v + \eta^h, \quad \eta^v \in \mathcal{V}_\Theta, \quad \eta^h \in \mathcal{H}_\Theta.$$

Since $\eta^v \in \mathcal{V}_\Theta$, there exists $X \in \text{Skew}(n)$ such that

$$\eta^v = (-XA + AX, -XB, CX).$$

Thus, η^h can be described as

$$\eta^h = (a + XA - AX, b + XB, c - CX).$$

Because $\eta^h \in \mathcal{H}_\Theta$, we obtain that

$$\begin{aligned} & \text{sk}(2(a + XA - AX)A^{-1} + B(b + XB)^\top \\ & + C^\top(c - CX)) = 0. \end{aligned}$$

It follows from this equation that (31) holds, because $a^\top = a$ and $X^\top = -X$.

E. Proof of Theorem 3

Using the Kronecker product and vec-operator, the operators \mathcal{L}_0 and \mathcal{L}_1 have the matrix representations $K_0 = A^{-1} \otimes A + A \otimes A^{-1} - 2I_{n^2}$ and $K_1 = I_n \otimes (BB^\top + C^\top C) + (BB^\top + C^\top C) \otimes I_n$. Both are symmetric, and K_1 is positive semidefinite [49]. Thus, $\mathcal{L}_1 \geq 0$. Note also that both summands of K_1 and thus of \mathcal{L}_1 are positive semidefinite, whence

$$\mathcal{L}_1(X) = 0 \Rightarrow (BB^\top + C^\top C)X = 0. \quad (77)$$

If $\lambda_j, \lambda_k \in \lambda(A)$ with corresponding orthonormal eigenvectors v_j, v_k , then

$$\mathcal{L}_0(v_j v_k^\top) = \mu_{jk} v_j v_k^\top,$$

where $\mu_{jk} := \frac{(\lambda_j - \lambda_k)^2}{\lambda_j \lambda_k}$. From the n orthonormal eigenvectors v_j , $j = 1, 2, \dots, n$, of the matrix A , we thus obtain n^2 orthonormal eigenvectors $v_j v_k^\top$, $j, k = 1, 2, \dots, n$, of the linear matrix mapping. Because $\mu_{jk} \geq 0$ for all j, k , it follows that $\mathcal{L}_0 \geq 0$. Together with $\mathcal{L}_1 \geq 0$, this implies that

$$\text{Ker } \mathcal{L} = \text{Ker } \mathcal{L}_1 \cap \text{Ker } \mathcal{L}_0. \quad (78)$$

See Fact 8.7.3 in [50]. Moreover, the kernel of \mathcal{L}_0 is spanned by the matrices $v_j v_k^\top + v_k v_j^\top$ and $v_j v_k^\top - v_k v_j^\top$ with $\lambda_j = \lambda_k$, $j, k = 1, 2, \dots, n$. That is,

$$\text{Ker } \mathcal{L}_0 \cap \text{Skew}(n) = \text{span}\{v_j v_k^\top - v_k v_j^\top \mid \lambda_j = \lambda_k\}.$$

The matrix A can be expressed as

$$A = V \text{diag}(\lambda_{n_1} I_{n_1}, \lambda_{n_2} I_{n_2}, \dots, \lambda_{n_l} I_{n_l}) V^\top,$$

where $n_1 + n_2 + \dots + n_l = n$, $\lambda_1 = \dots = \lambda_{n_1} < \lambda_{n_1+1} = \dots = \lambda_{n_2} < \dots < \lambda_{n_1+n_2+\dots+n_{l-1}+1} = \dots = \lambda_{n_l}$, and after suitable ordering and partitioning, $V = (V_1 \dots V_l) = (v_1 \dots v_n)$ is orthogonal with $\text{Im } V_j = \text{Ker}(\lambda_{n_j} I_n - A)$. We thus obtain that

$$\begin{aligned} & \text{Ker } \mathcal{L}_0 \cap \text{Skew}(n) \\ & = \{V \text{diag}(S_1, S_2, \dots, S_l) V^\top \mid S_j \in \text{Skew}(n_j)\}. \end{aligned}$$

To see this, note that the right hand side is the linear subspace of $\text{Skew}(n)$, spanned by

$$v_j v_k^\top - v_k v_j^\top = V(e_j e_k^\top - e_k e_j^\top) V^\top,$$

where $\lambda_j = \lambda_k$ and e_j is the j -th unit vector in \mathbf{R}^n . Thus, it follows from (77) and (78) that $U \in \text{Ker } \mathcal{L} \cap \text{Skew}(n)$ implies $U = V \text{diag}(S_1, S_2, \dots, S_l) V^\top$ with $(BB^\top + C^\top C)U = 0$. In particular, we have that

$$\begin{cases} 0 = B^\top U V_j = B^\top V_j S_j \\ 0 = C U V_j = C V_j S_j \end{cases}$$

for $j = 1, 2, \dots, l$, and thus

$$\text{Ker}(\lambda_{n_j} I_n - A) \cap \text{Ker } B^\top \cap \text{Ker } C \supset \text{Im}(V_j S_j).$$

Therefore,

$$\dim(\text{Ker}(\lambda_{n_j} I_n - A) \cap \text{Ker } B^\top \cap \text{Ker } C) \geq \text{rank } S_j. \quad (79)$$

Because each $S_j \in \text{Skew}(n_j)$ necessarily has even rank, assumption (32) and (79) yield that $\text{rank } S_j = 0$ for $j = 1, 2, \dots, l$, whence $U = 0$. This implies that

$$\text{Ker } \mathcal{L} \cap \text{Skew}(n) = \{0\}, \quad (80)$$

or equivalently $\text{Ker } \mathcal{L} \subset \text{Sym}(n)$. Eq. (80) implies that $\mathcal{L} : \text{Skew}(n) \rightarrow \text{Skew}(n)$ is an automorphism.

REFERENCES

- [1] F. Dörfler, J. W. Simpson-Porco, and F. Bullo, "Electrical networks and algebraic graph theory: Models, properties, and applications," *Proceedings of the IEEE*, vol. 106, no. 5, pp. 977–1005, 2018.
- [2] L. Vandenberghe, S. Boyd, and A. El Gamal, "Optimal wire and transistor sizing for circuits with non-tree topology," in *Proceedings of the 1997 IEEE/ACM international conference on Computer-aided design*. IEEE Computer Society, 1997, pp. 252–259.
- [3] J. C. Willems, "Realization of systems with internal passivity and symmetry constraints," *Journal of the Franklin Institute*, vol. 301, no. 6, pp. 605–621, 1976.
- [4] M. Mesbahi and M. Egerstedt, *Graph Theoretic Methods in Multiagent Networks*. Princeton University Press, 2010.
- [5] R. Olfati-Saber and R. M. Murray, "Consensus problems in networks of agents with switching topology and time-delays," *IEEE Transactions on Automatic Control*, vol. 49, no. 9, pp. 1520–1533, 2004.
- [6] T. Hatanaka, X. Zhang, W. Shi, M. Zhu, and N. Li, "Physics-integrated hierarchical/distributed HVAC optimization for multiple buildings with robustness against time delays," in *IEEE 56th Annual Conference on Decision and Control (CDC)*, 2017, pp. 6573–6579.

- [7] C. Lidström and A. Rantzer, "Optimal H^∞ state feedback for systems with symmetric and Hurwitz state matrix," in *American Control Conference (ACC)*, 2016, pp. 3366–3371.
- [8] B. Hanzon and R. L. M. Peeters, "On the Riemannian interpretation of the Gauss-Newton algorithm," in *Mutual impact of computing power and control theory*. Springer, 1993, pp. 111–121.
- [9] L. Ljung, *System Identification: Theory for the User*. Prentice-Hall, 1999.
- [10] T. Mckelvey, A. Helmersson, and T. Ribarits, "Data driven local coordinates for multivariable linear systems and their application to system identification," *Automatica*, vol. 40, no. 9, pp. 1629–1635, 2004.
- [11] R. Peeters, *System identification based on Riemannian geometry: theory and algorithms*. Thesis Publishers Amsterdam, 1994.
- [12] H. Sato and K. Sato, "Riemannian Optimal System Identification Algorithm for Linear MIMO Systems," *IEEE Control Systems Letters*, vol. 1, no. 2, pp. 376–381, 2017.
- [13] A. Wills and B. Ninness, "On gradient-based search for multivariable system estimates," *IEEE Transactions on Automatic Control*, vol. 53, no. 1, pp. 298–306, 2008.
- [14] T. Katayama, *Subspace Methods for System Identification*. Springer Science & Business Media, 2006.
- [15] W. E. Larimore, "Canonical variate analysis in identification, filtering, and adaptive control," in *Proceedings of the 29th IEEE Conference on Decision and Control*, 1990, pp. 596–604.
- [16] S. J. Qin, "An overview of subspace identification," *Computers & Chemical Engineering*, vol. 30, no. 10, pp. 1502–1513, 2006.
- [17] P. Van Overschee and B. De Moor, "N4SID: Subspace algorithms for the identification of combined deterministic-stochastic systems," *Automatica*, vol. 30, no. 1, pp. 75–93, 1994.
- [18] —, "A unifying theorem for three subspace system identification algorithms," *Automatica*, vol. 31, no. 12, pp. 1853–1864, 1995.
- [19] M. Verhaegen and P. Dewilde, "Subspace model identification part 1. The output-error state-space model identification class of algorithms," *International Journal of Control*, vol. 56, no. 5, pp. 1187–1210, 1992.
- [20] M. Verhaegen and A. Hansson, "N2SID: Nuclear norm subspace identification of innovation models," *Automatica*, vol. 72, pp. 57–63, 2016.
- [21] M. C. Campi, T. Sugie, and F. Sakai, "An iterative identification method for linear continuous-time systems," *IEEE Transactions on Automatic Control*, vol. 53, no. 7, pp. 1661–1669, 2008.
- [22] H. Garnier, M. Gilson, T. Bastogne, and M. Mensler, "The contsid toolbox: A software support for data-based continuous-time modelling," in *Identification of Continuous-Time Models from Sampled Data*. Springer, 2008, pp. 249–290.
- [23] M. Johansson, R. and Verhaegen and C. T. Chou, "Stochastic theory of continuous-time state-space identification," *IEEE Transactions on Signal Processing*, vol. 47, no. 1, pp. 41–51, 1999.
- [24] I. Maruta and T. Sugie, "Projection-based identification algorithm for grey-box continuous-time models," *Systems & Control Letters*, vol. 62, no. 11, pp. 1090–1097, 2013.
- [25] A. Ohsumi, K. Kameyama, and K. Yamaguchi, "Subspace identification for continuous-time stochastic systems via distribution-based approach," *Automatica*, vol. 38, no. 1, pp. 63–79, 2002.
- [26] P. Van Overschee and B. De Moor, "Continuous-time frequency domain subspace system identification," *Signal Processing*, vol. 52, no. 2, pp. 179–194, 1996.
- [27] S. Lang, *Fundamentals of differential geometry*. Springer Science & Business Media, 2012, vol. 191.
- [28] K. Sato and H. Sato, "Structure-preserving H^2 optimal model reduction based on Riemannian trust-region method," *IEEE Transactions on Automatic Control*, vol. 63, no. 2, pp. 505–511, 2018.
- [29] H. Akaike, "A new look at the statistical model identification," *IEEE Transactions on Automatic Control*, vol. 19, no. 6, pp. 716–723, 1974.
- [30] M. Verhaegen, "Identification of the deterministic part of MIMO state space models given in innovations form from input-output data," *Automatica*, vol. 30, no. 1, pp. 61–74, 1994.
- [31] K. Tan and K. M. Grigoriadis, "Stabilization and H^∞ control of symmetric systems: an explicit solution," *Systems & Control Letters*, vol. 44, no. 1, pp. 57–72, 2001.
- [32] P.-A. Absil, R. Mahony, and R. Sepulchre, *Optimization Algorithms on Matrix Manifolds*. Princeton University Press, 2008.
- [33] A. Edelman, T. A. Arias, and S. T. Smith, "The geometry of algorithms with orthogonality constraints," *SIAM journal on Matrix Analysis and Applications*, vol. 20, no. 2, pp. 303–353, 1998.
- [34] U. Helmke and J. B. Moore, *Optimization and dynamical systems*. Springer-Verlag London, 1994.
- [35] J. M. Lee, *Introduction to Smooth Manifolds*. Springer, 2013.
- [36] B. Afsari and R. Vidal, "Bundle reduction and the alignment distance on spaces of state-space LTI systems," *IEEE Transactions on Automatic Control*, vol. 62, no. 8, pp. 3804–3819, 2017.
- [37] R. Brockett, "Some geometric questions in the theory of linear systems," *IEEE Transactions on Automatic Control*, vol. 21, no. 4, pp. 449–455, 1976.
- [38] D. F. Delchamps, "Global structure of families of multivariable linear systems with an application to identification," *Mathematical systems theory*, vol. 18, no. 1, pp. 329–380, 1985.
- [39] B. Hanzon and R. J. Ober, "Overlapping block-balanced canonical forms for various classes of linear systems," *Linear Algebra and its Applications*, vol. 281, no. 1-3, pp. 171–225, 1998.
- [40] M. Hazewinkel, "Moduli and canonical forms for linear dynamical systems II: The topological case," *Mathematical Systems Theory*, vol. 10, no. 1, pp. 363–385, 1977.
- [41] E. D. Sontag, *Mathematical control theory: deterministic finite dimensional systems*. Springer, 1998, vol. 6.
- [42] S. Sra and R. Hosseini, "Conic geometric optimization on the manifold of positive definite matrices," *SIAM Journal on Optimization*, vol. 25, no. 1, pp. 713–739, 2015.
- [43] H. Sato, "A Dai-Yuan-type Riemannian conjugate gradient method with the weak Wolfe conditions," *Computational Optimization and Applications*, vol. 64, no. 1, pp. 101–118, 2016.
- [44] W. Ring and B. Wirth, "Optimization methods on Riemannian manifolds and their application to shape space," *SIAM Journal on Optimization*, vol. 22, no. 2, pp. 596–627, 2012.
- [45] S. Amari, "Natural gradient works efficiently in learning," *Neural computation*, vol. 10, no. 2, pp. 251–276, 1998.
- [46] A. J. M. Van Overbeek and L. Ljung, "On-line structure selection for multivariable state-space models," *Automatica*, vol. 18, no. 5, pp. 529–543, 1982.
- [47] D. J. Watts and S. H. Strogatz, "Collective dynamics of 'small-world' networks," *nature*, vol. 393, no. 6684, pp. 440–442, 1998.
- [48] S. T. Smith, "Covariance, subspace, and intrinsic Cramér-Rao bounds," *IEEE Transactions on Signal Processing*, vol. 53, no. 5, pp. 1610–1630, 2005.
- [49] A. C. Antoulas, *Approximation of Large-Scale Dynamical Systems*. SIAM, 2005.
- [50] D. S. Bernstein, *Matrix Mathematics: Theory, Facts, and Formulas*. Princeton and Oxford: Princeton University Press, 2009.